

INTEGRAL observations of Gamma-Ray Bursts polarization

P. Laurent, F. Lebrun (APC)



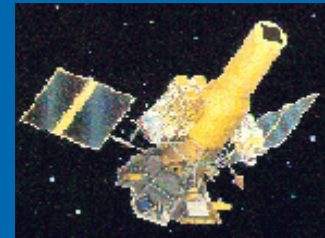
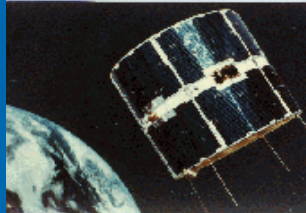
plan

1. Description of the INTEGRAL observatory.
2. Polarimetry with INTEGRAL.
3. Observation of polarization in Gamma-Ray Bursts.

The INTEGRAL observatory

High-energy astrophysics: Past and present

COS-B
1975-1982
(100 MeV gamma-rays)



GRANAT/SIGMA
1989-1997
(soft gamma-rays)

The golden age

XMM-Newton
1999-



Fermi
2008-

INTEGRAL
2002-



HESS
2003-



October 17th, 2002



November, 7th 2012

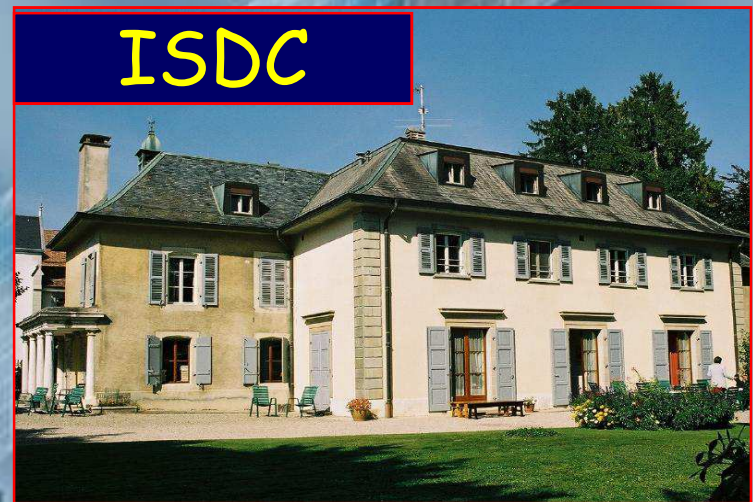
INTEGRAL Scientific payload

Satellite
4.1 tons
5 m height
3.7 m diameter
Launched in 2002

OMC (optical)

IBIS
15 keV - 10 MeV
12' FWHM imaging
<1' source location
19°x19° FOV

JEM-X



SPI
20 keV - 8 MeV
2 keV FWHM
26° Ø FOV

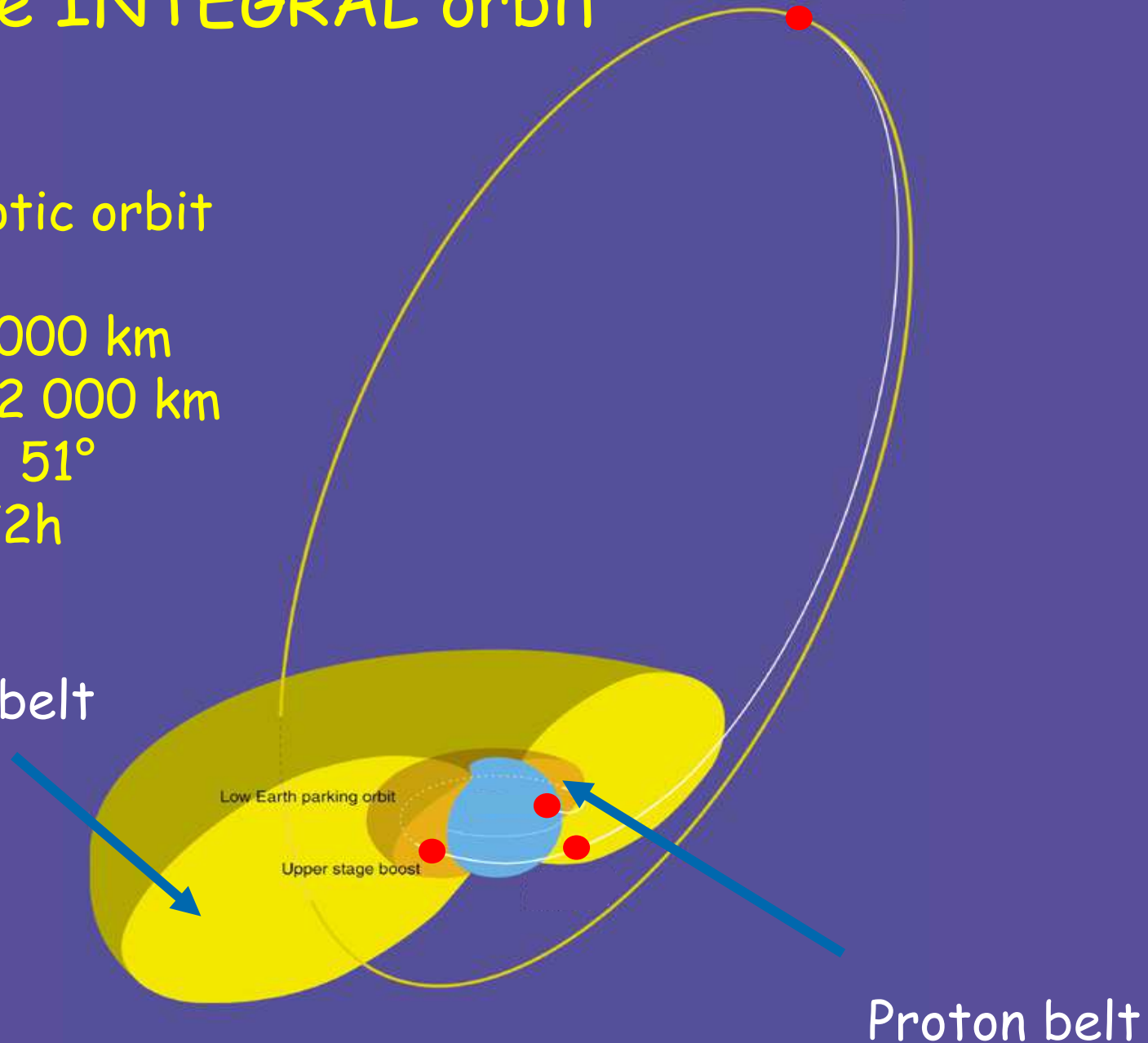


The INTEGRAL orbit

Highly elliptic orbit

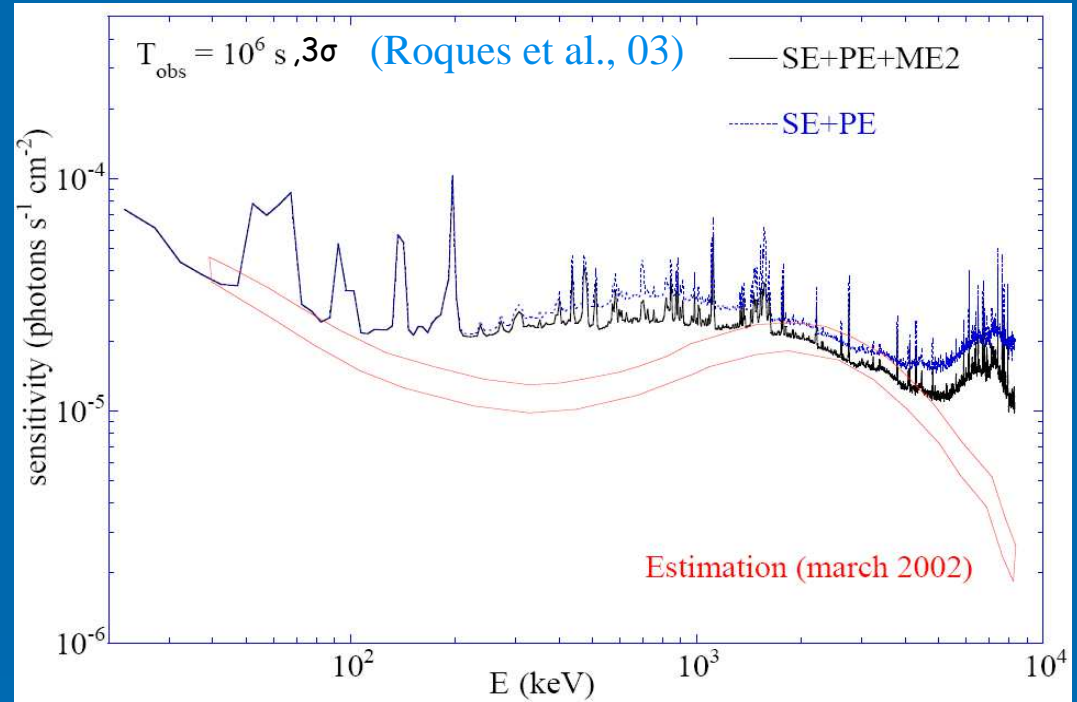
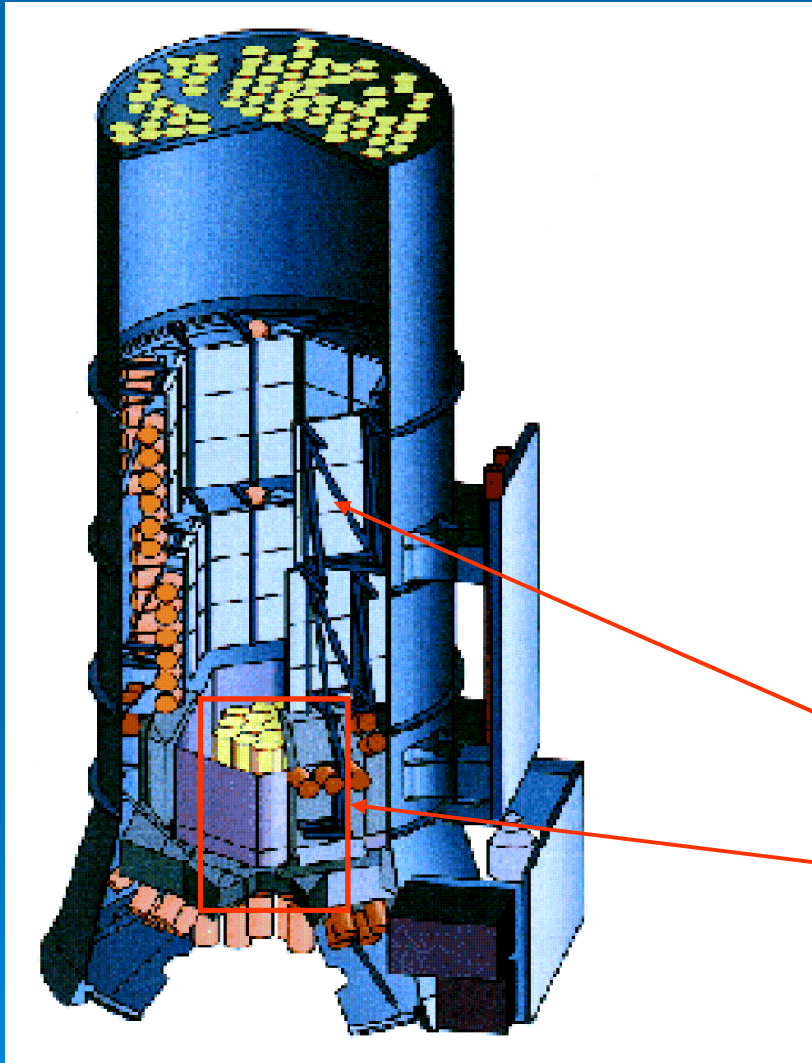
Apogee: 13 000 km
Perigee : 152 000 km
Inclination : 51°
Duration : 72h

Electron belt





The INTEGRAL spectrometer: SPI



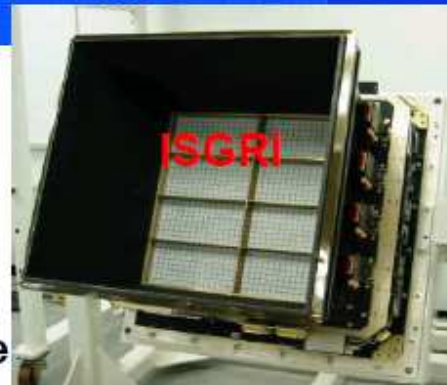
BGO anticoincidence (700 kg)
19 Ge diodes, $T \sim 80 \text{ K}$
 $\Delta E \sim 2 \text{ keV} @ 1 \text{ MeV} - 500 \text{ cm}^2$



The INTEGRAL Imager : IBIS



IBIS detector assembly:
two stacked detection
planes, lateral and
bottom veto
anticoincidence, passive
tungsten shield



**coded mask, placed 3.2m
above detector (1m²)**

Collection area ~ 3000 cm²

Two-Layers detector:

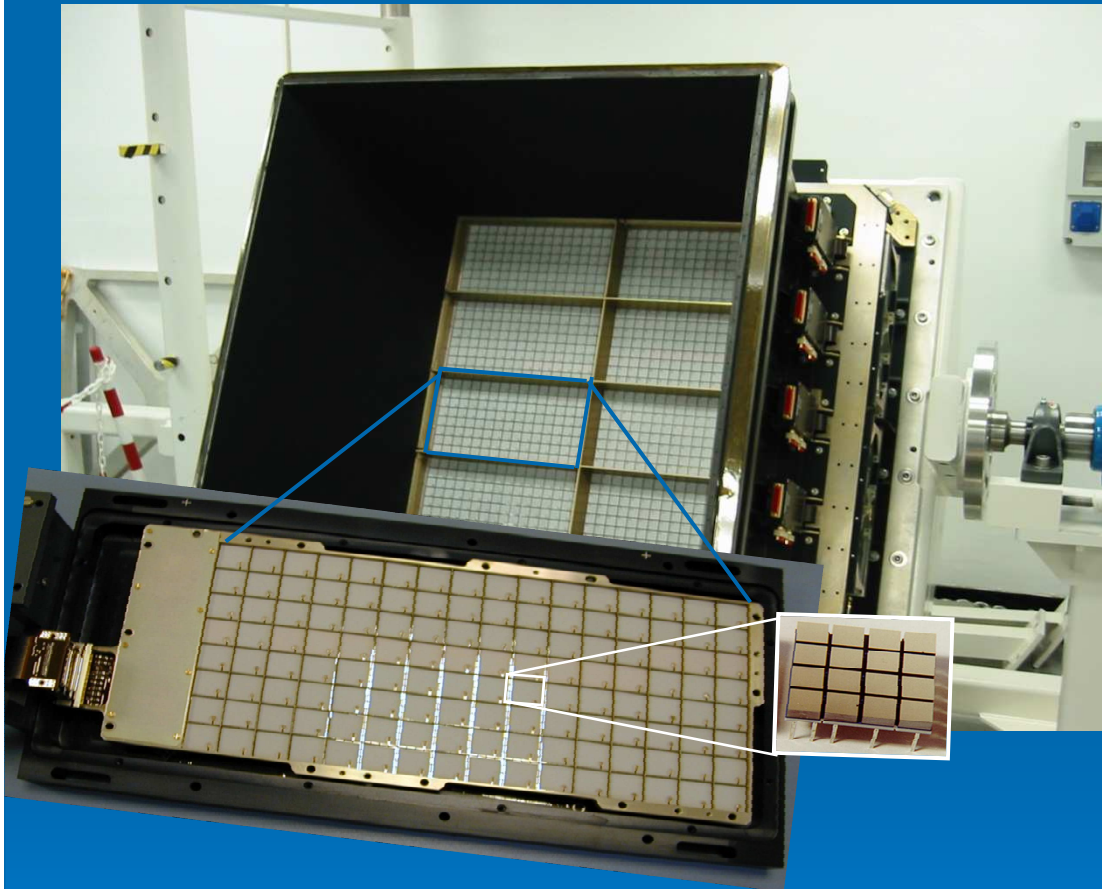
1) 2mm thick CdTe (ISGRI)

2) 30mm thick CsI (PICsIT)

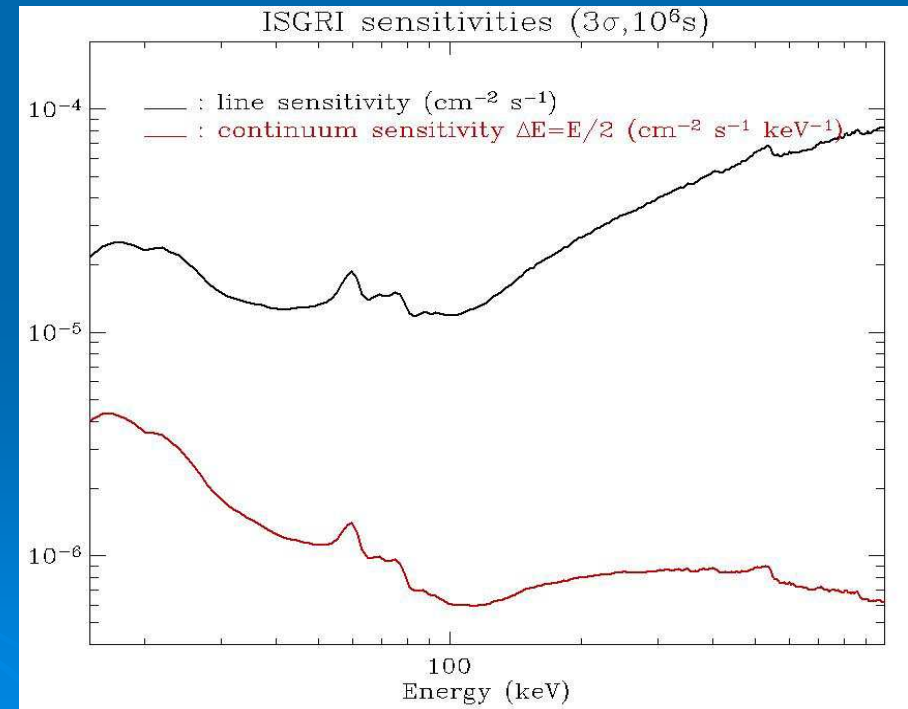
Field-of-view: $\pm 14.5^\circ$ FWZR (\pm
4.5° fully coded)



The ISGRI position sensitive detector



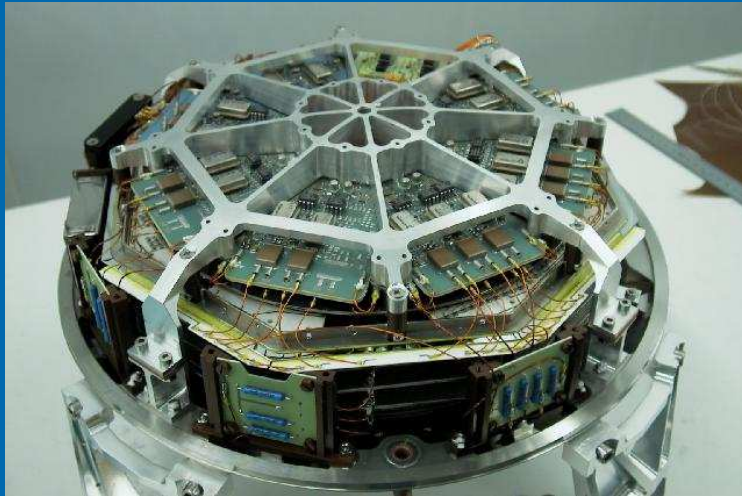
- 16384 CdTe pixels (2620 cm^2)
- FWHM = 9 keV at 60 keV
- Spatial resolution: 4.6 mm
- Timing accuracy:
 - relative: 254 ns
 - absolute: 100 μs
- Up to $60\,000 \text{ s}^{-1}$



First ambient-temperature
semiconductor gamma-camera
in the world !



The INTEGRAL X-ray monitor: JEM-X



- JEM-X provides images with arcminute angular resolution in the 3 - 35 keV energy band.
- The baseline photon detection system consists of two identical high pressure imaging microstrip gas chambers (1.5 bar, 90% Xenon + 10% Methane).
- Each detector unit views the sky through its coded aperture mask located at a distance of ~ 3.2 m above the detection plane.



The INTEGRAL Optical Monitor: OMC



- The Optical Monitoring Camera OMC consists of a passively cooled CCD (2055 x 1056 pixels, imaging area: 1024 x 1024 pixels) working in frame transfer mode.
- The CCD is located in the focal plane of a 50 mm (diameter) lens including a Johnson V-filter to cover the 500 - 600 nm wavelength range.
- The OMC is mounted close to the top of the payload module structure, and observes the optical emission from the prime targets of the INTEGRAL main gamma-ray instruments.



The INTEGRAL Science Data Center

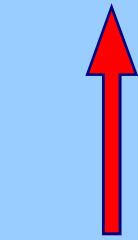
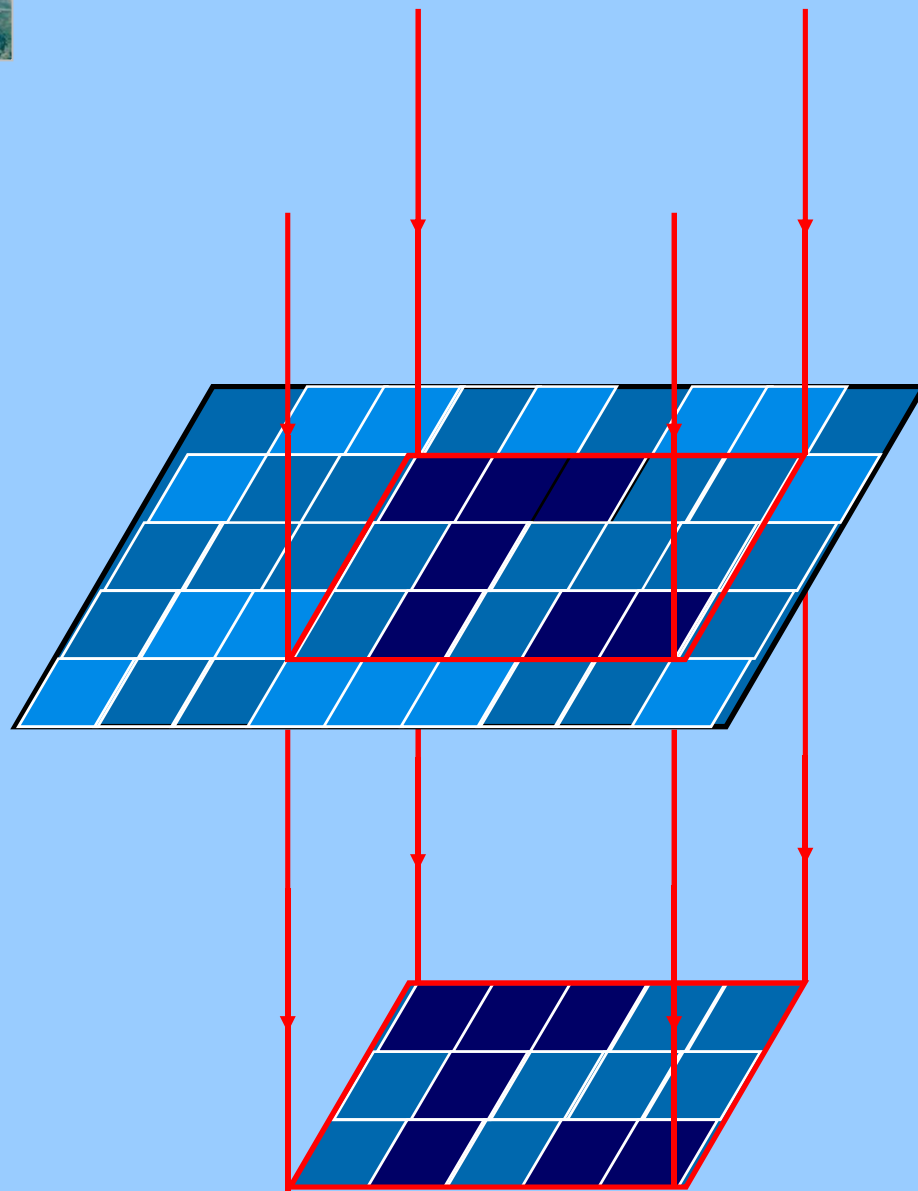


- The task of ISDC is to be the interface between the INTEGRAL satellite and the scientific community worldwide. It is located in Versoix, near Geneva and is attached to the University of Geneva.
- It is responsible for the analysis and processing of INTEGRAL data, which are made directly usable by scientists.
- Jointly to the instrument teams, it also provides to the scientific community software for the data exploitation. The ISDC maintains the INTEGRAL archive accessible on the internet.

The coded mask imaging technique



Totally coded field of view



source 1

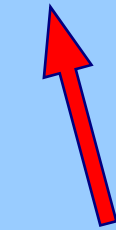
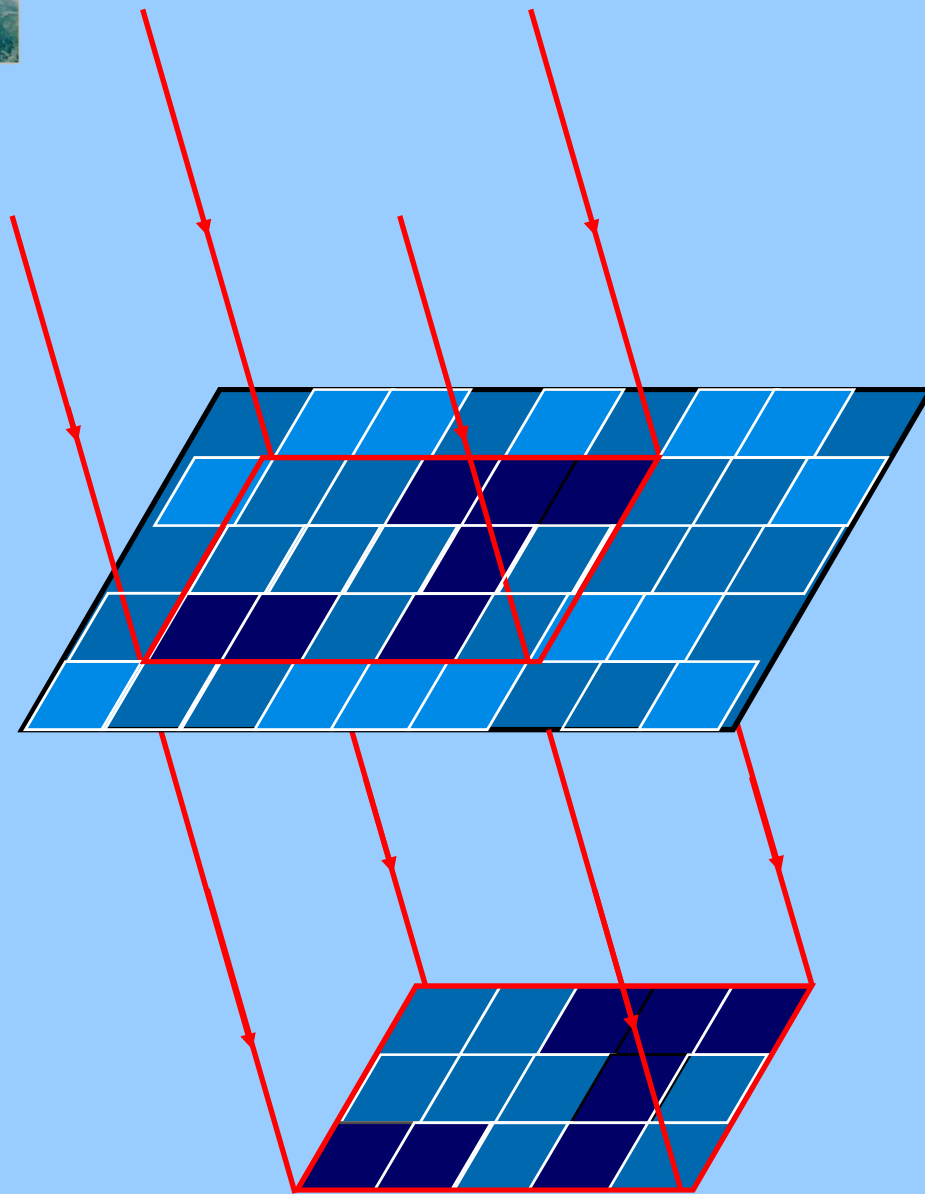
at infinity

Coded mask

Position sensitive
detector
(e.g. ISGRI)



Totally coded field of view



source 2

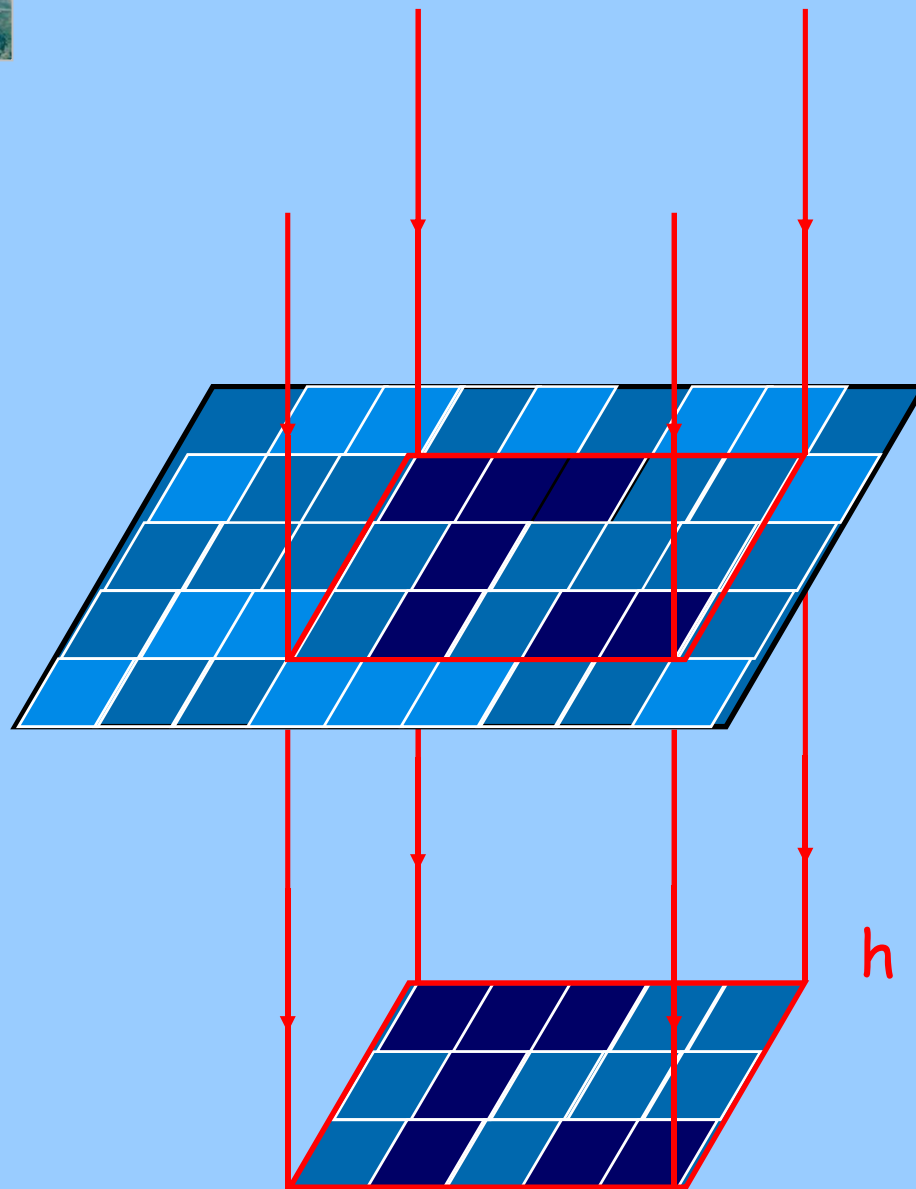
at infinity

Coded mask

Position sensitive
detector
(e.g. ISGRI)



Totally coded field of view



↑
source 1
at infinity

Coded mask

$$\delta\theta = \arctg\left(\frac{m}{h}\right)$$

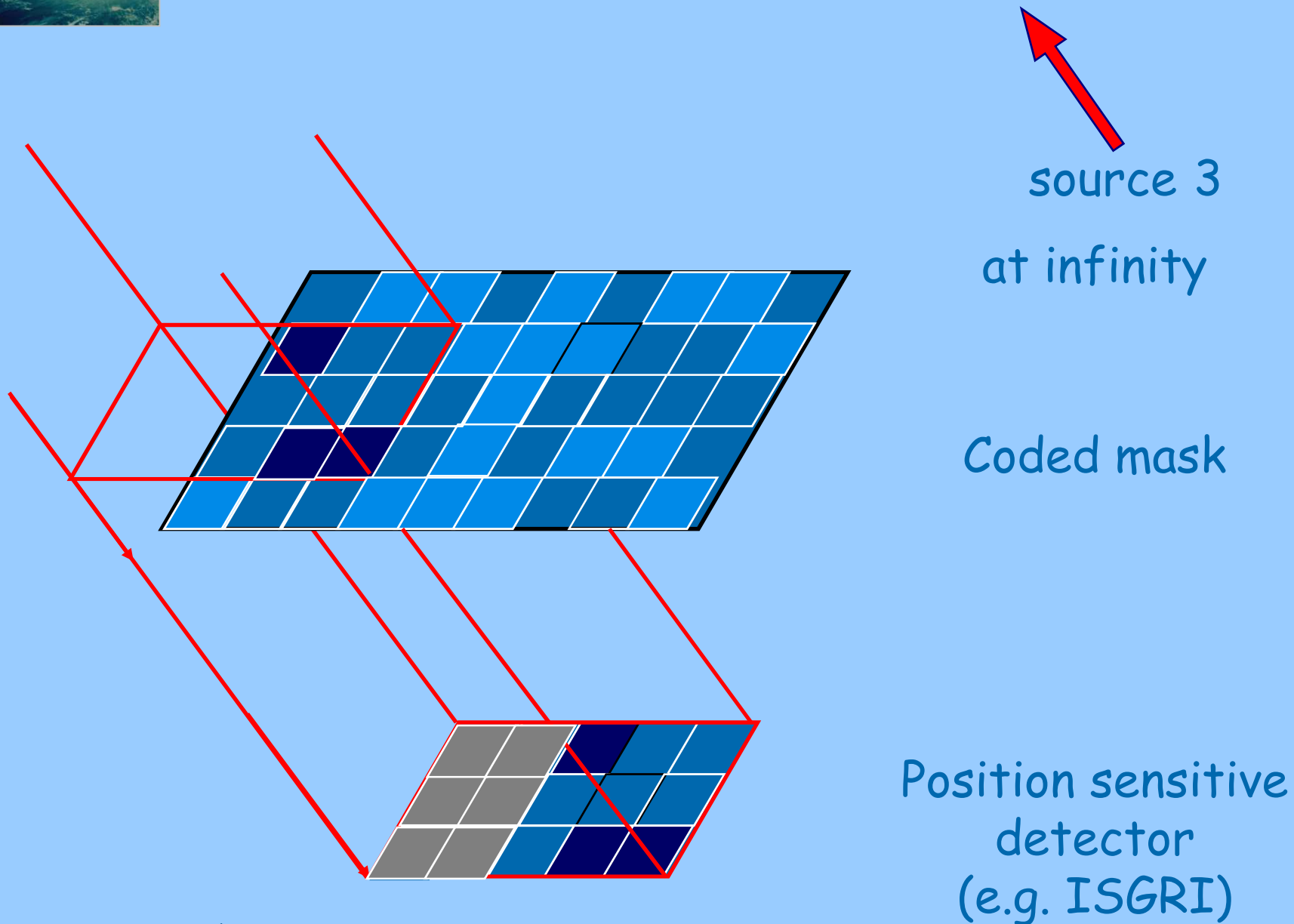
m : mask element size

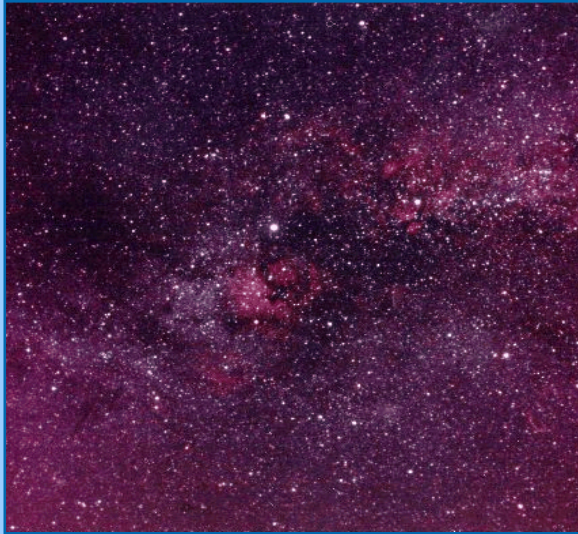
h : mask - detector distance

Position sensitive
detector
(e.g. ISGRI)

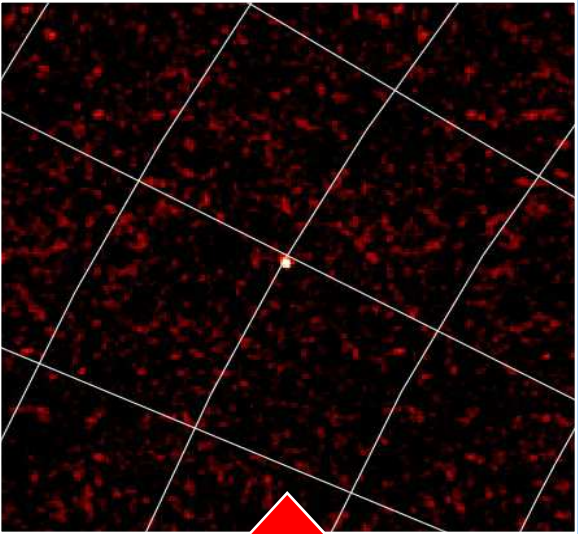


Partially coded field of view

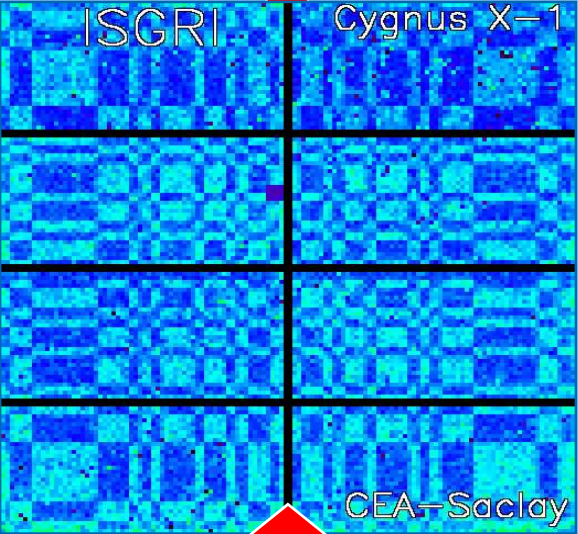




observation

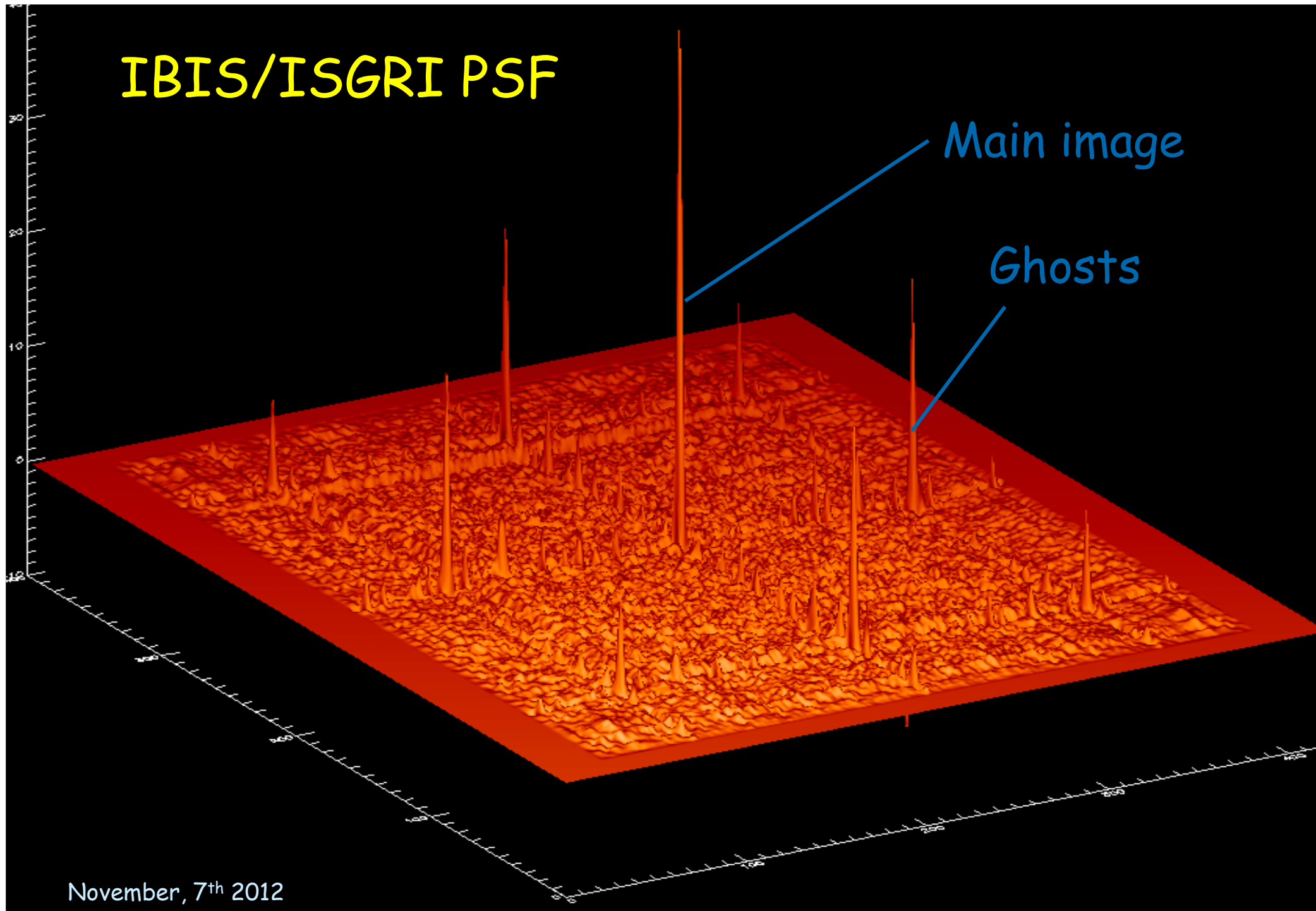


decoding



transmission

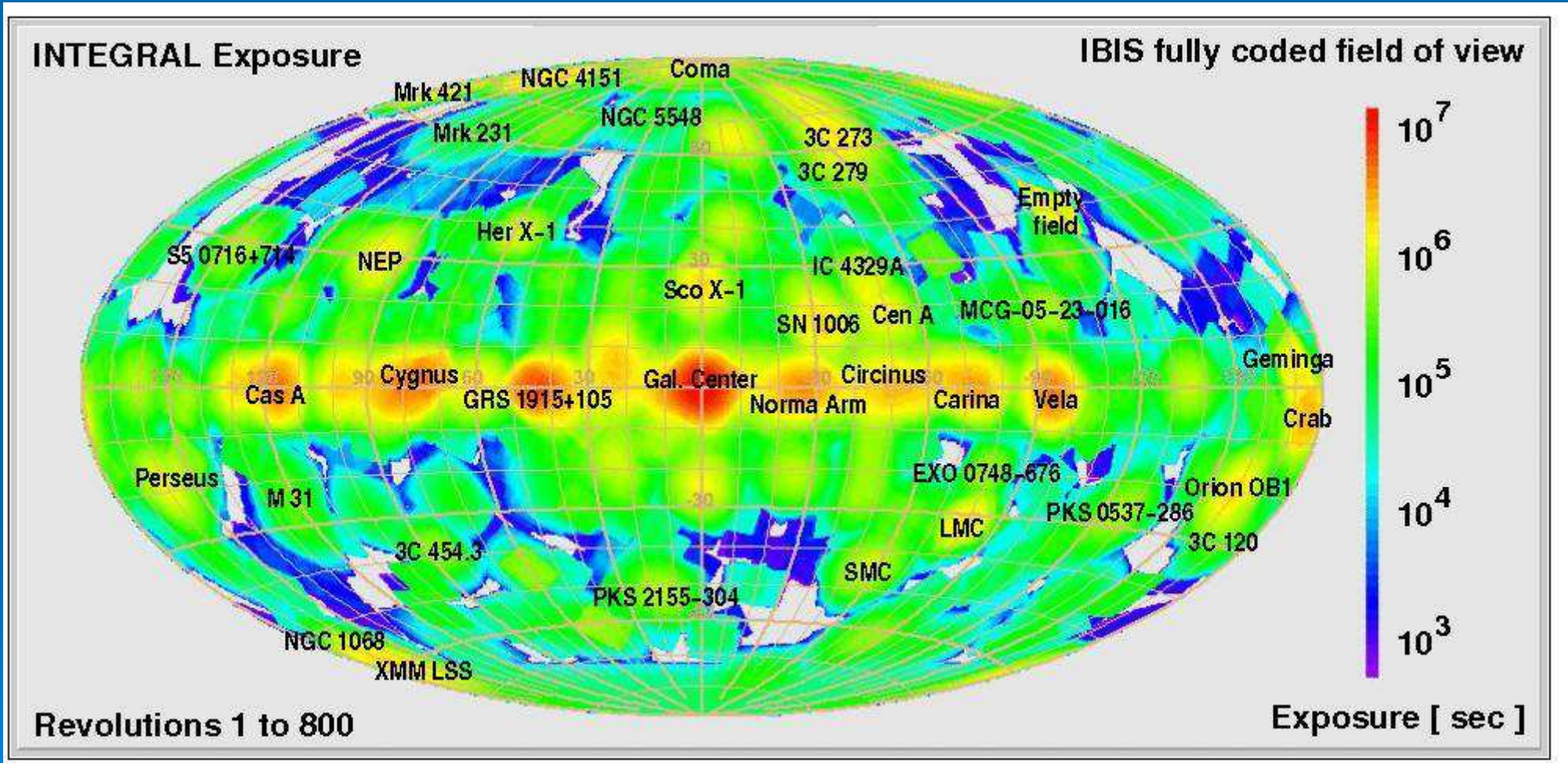
IBIS/ISGRI PSF



November, 7th 2012

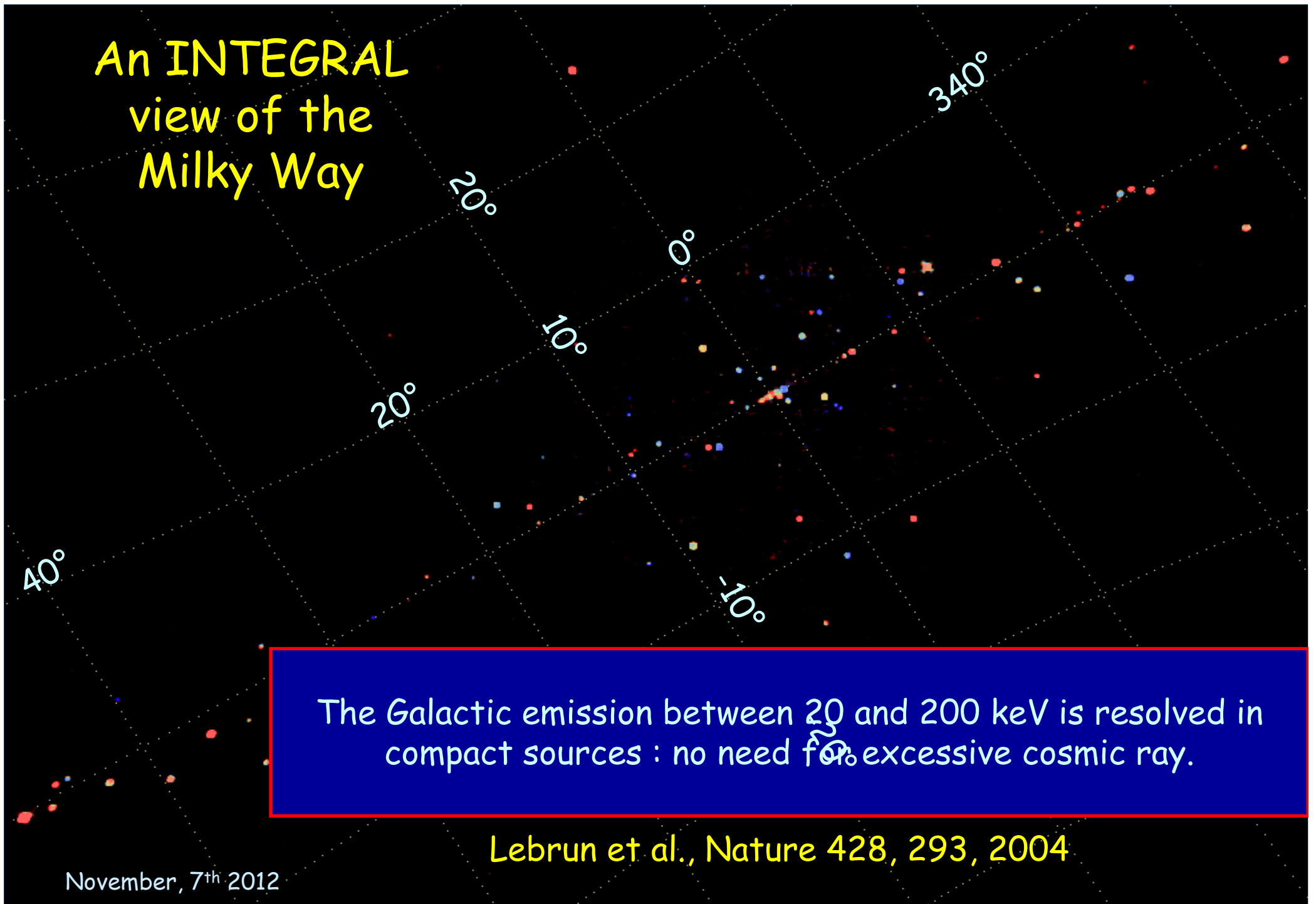


INTEGRAL sky coverage after 800 revolutions (~8 years)



Highlights of some INTEGRAL results

An INTEGRAL view of the Milky Way

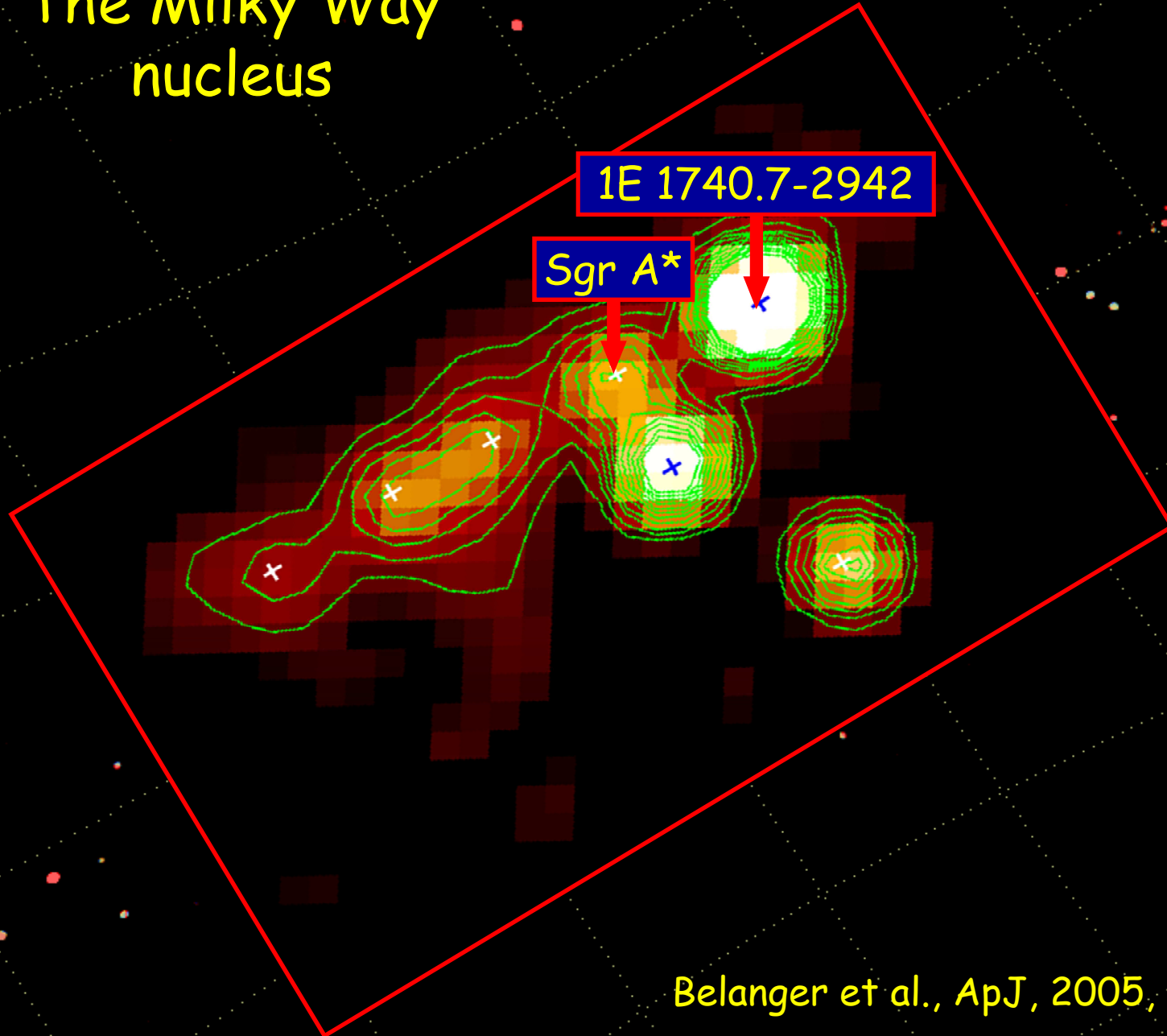


The Galactic emission between 20 and 200 keV is resolved in compact sources : no need for excessive cosmic ray.

Lebrun et al., Nature 428, 293, 2004



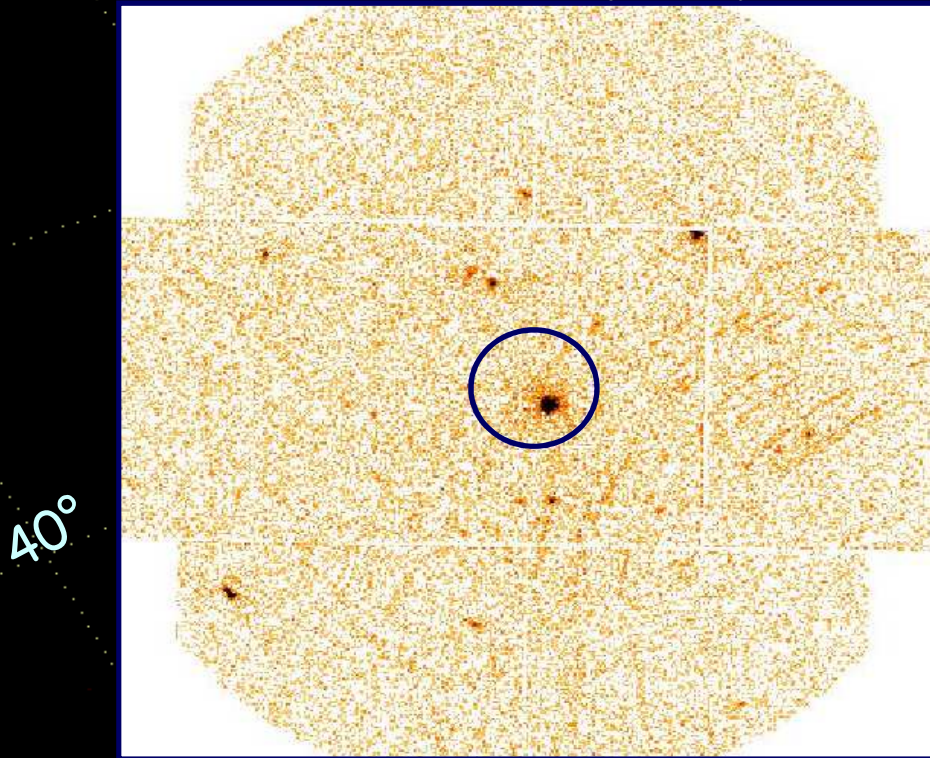
The Milky Way nucleus



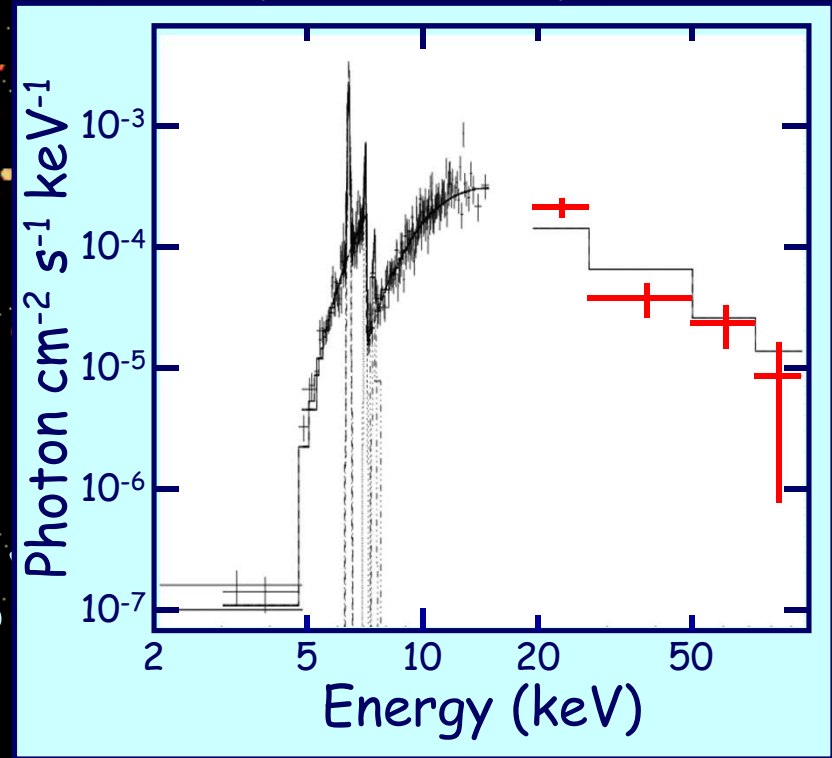
Belanger et al., ApJ, 2005, 635, 109



very absorbed X-ray binaries



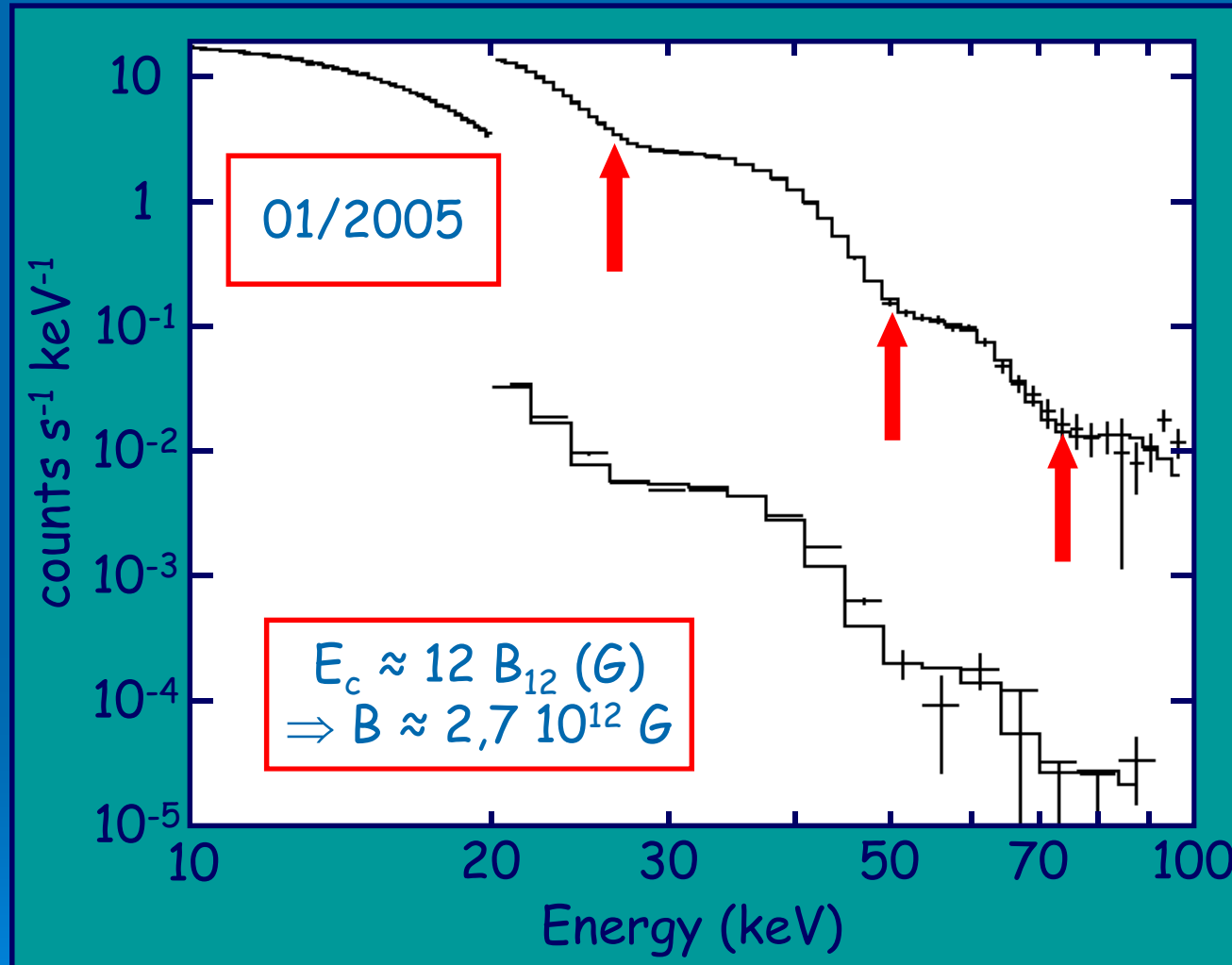
IGR J16318-4848



• Chaty et al., Ap&SS, 2005, 297, 235



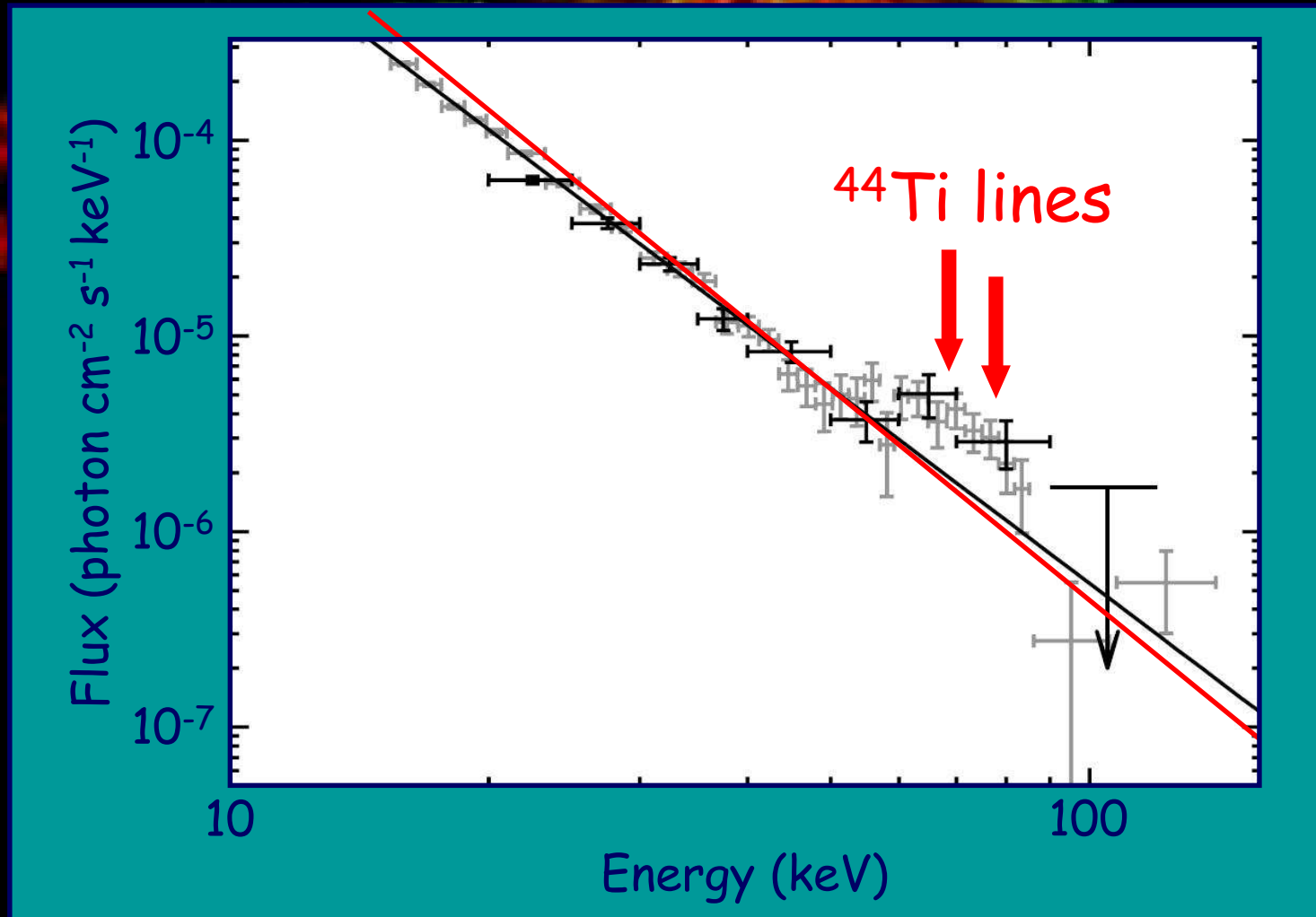
V0332+53 in outburst: cyclotron lines



Kreykenbohm et al., A&A, 2005, 433, L45



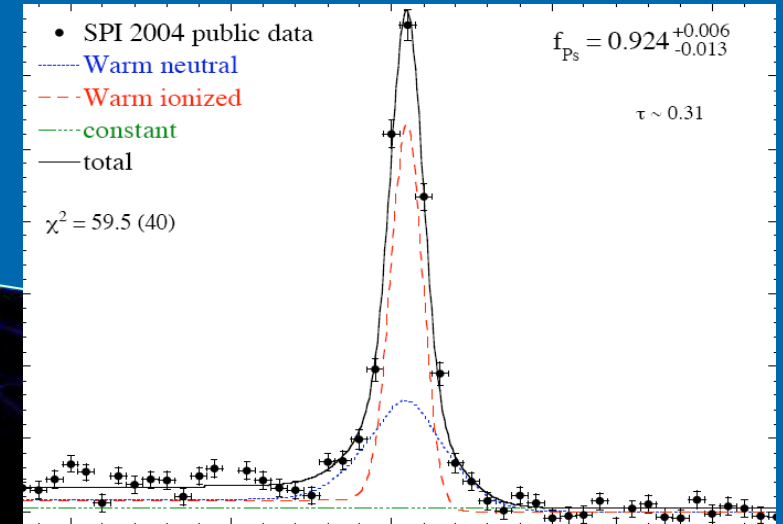
Cas A : the SNR shell type prototype



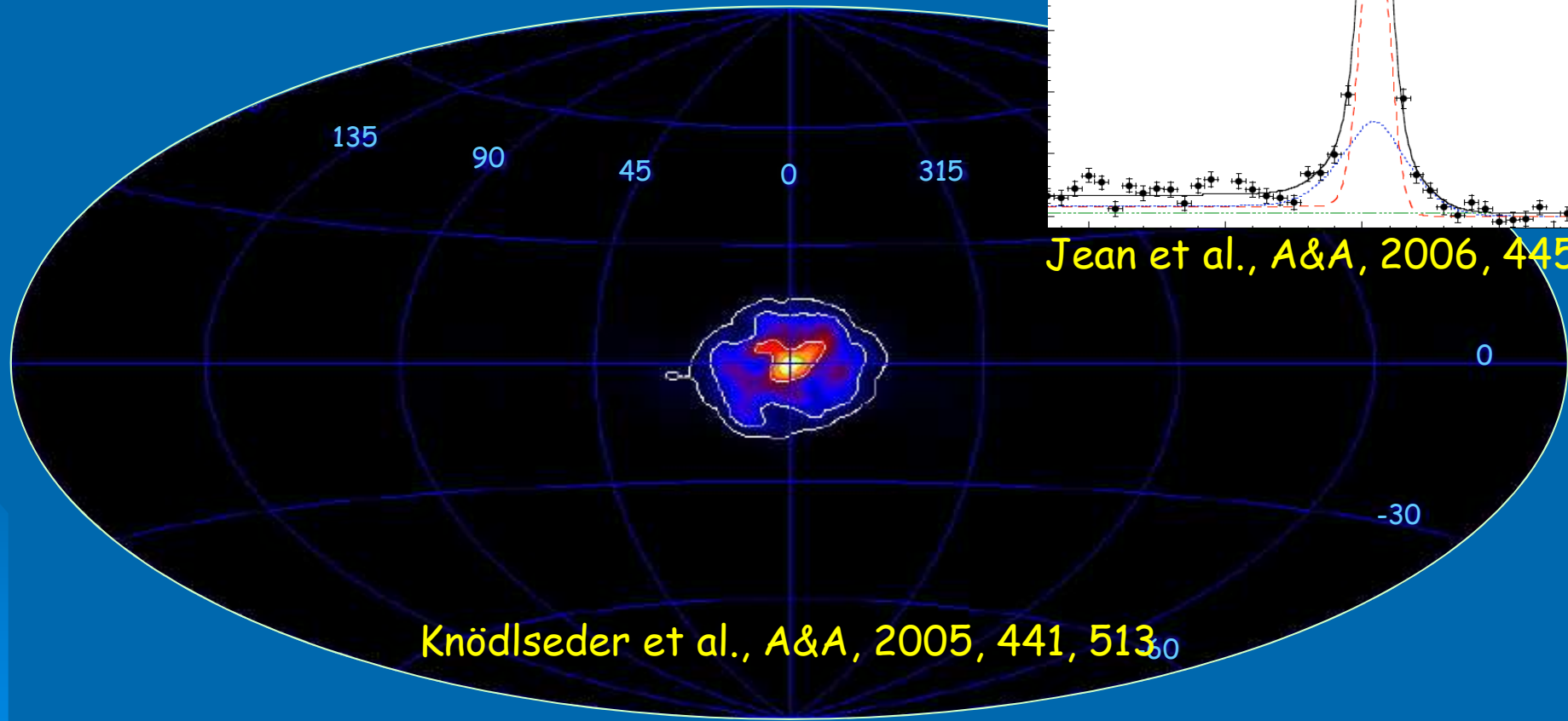
Renaud et al., ApJ, 2006, 647, L41



511 keV line emission from the Galaxy

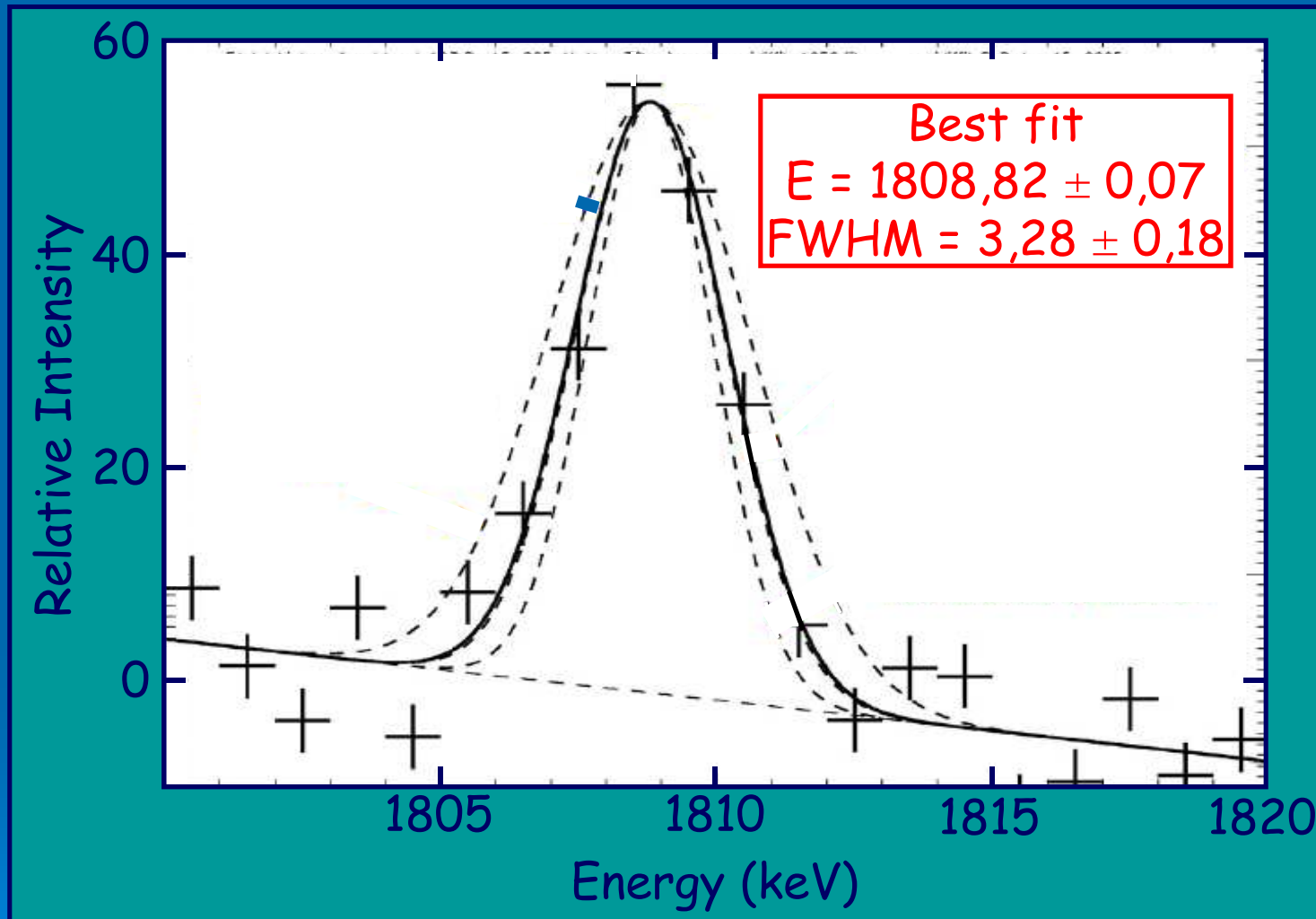


Jean et al., A&A, 2006, 445, 579





^{26}Al decay



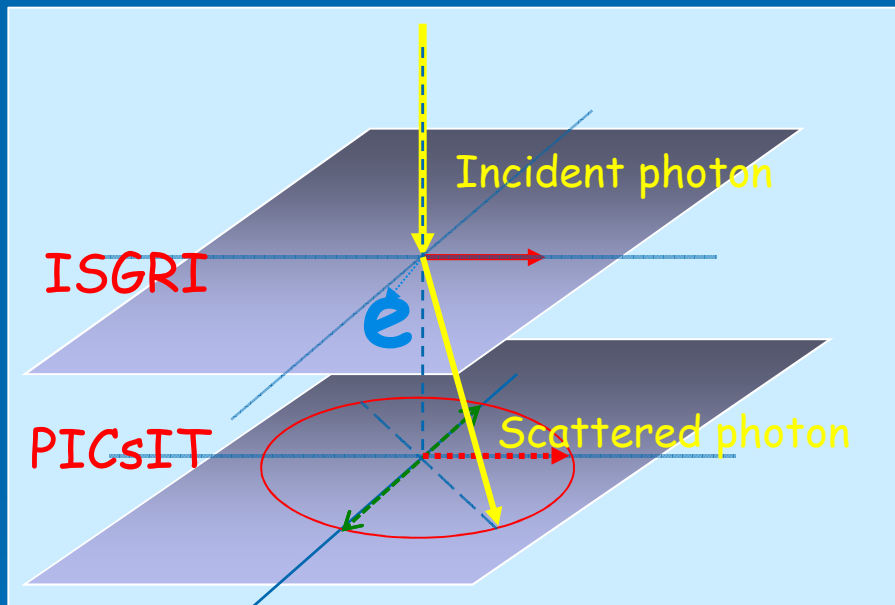
Diehl et al., *A&A*, 2006, 449, 102

Polarimetry with Integral

The INTEGRAL/IBIS Polarimeter



The IBIS/Compton telescope



- The IBIS telescope is a coded mask telescope which could be used as a Compton telescope.
- The Compton mode events are ISGRI and PICSIT events in temporal coincidence, within a window $\tau_w \approx 3.8 \mu\text{s}$.

- Within this window, chance coincidence, called hereafter “spurious events”, may also occur.



The IBIS/Compton telescope advantages

It is a coded mask Compton telescope, so it takes advantage of the two imaging techniques:

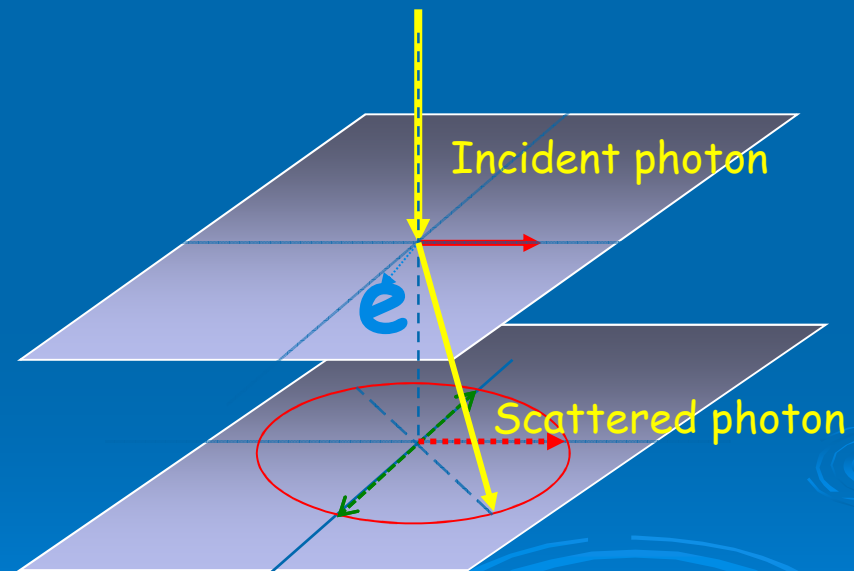
- It produces sky images using the coded mask with the same capabilities as ISGRI.
- It has an inherent very low background (~ 90 cts/s) compared to SPI and PiCsIT.
- We can use the Compton effect to further reduce the background, by selecting with the Compton kinetics, events coming only from the coded mask FOV.
- We can do polarimetry !



Compton polarimetry principles

Compton scattering cross section is **maximum** for photons scattered **at right angle** to the direction of the incident **electric vector** \Rightarrow asymmetry in the azimuthal profile S of scattered events.

$$S = \bar{S} \left[1 + a \cdot \cos(2(\varphi - \varphi_0)) \right]$$



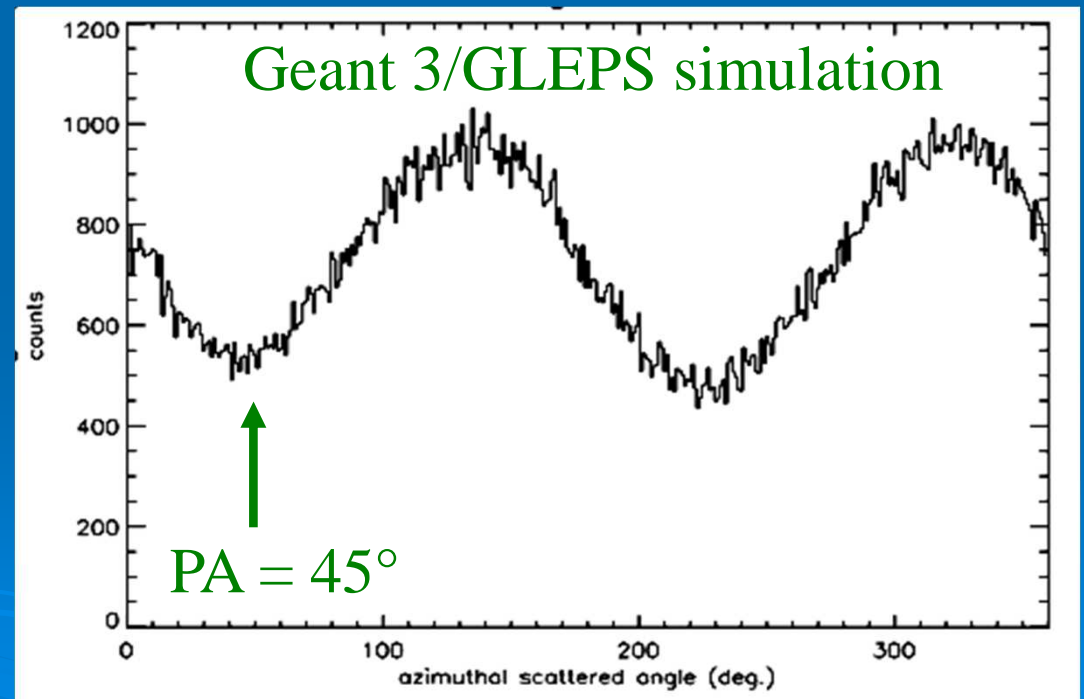


Compton polarimetry principles

$$S = \bar{S} \left[1 + a \cdot \cos(2(\varphi - \varphi_0)) \right]$$

modulation

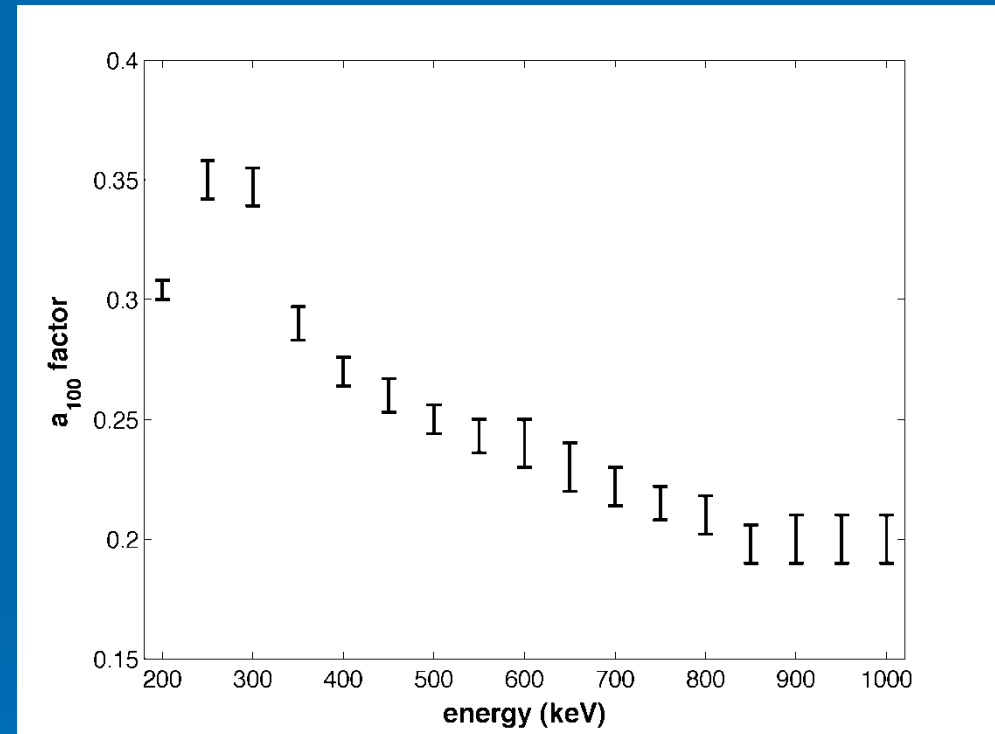
- a = modulation factor
- polar. fraction = PF = a/a_{100}
- a_{100} = modulation for a 100 % polarized source.
- polar. angle = PA = $\varphi_0 - \pi/2 + n\pi$





The a_{100} factor

- a_{100} necessary to estimate the pulse fraction.
- a_{100} estimate: GEANT 3/ GLEPS simulation for a 100 % linearly polarized source.
- $a_{100} = 0.304 \pm 0.003$ for a Crab-like spectrum
- No on-ground calibration.



↓
 a_{100} between 0.2 and 0.4

How is it described ?

- By a set of four quantities I,Q,U,V, called the Stokes parameters, which completely specify the nature of radiation from an astronomical source.
- Devised by Sir G. G. Stokes (1852) and adapted for astronomy by S. Chandrasekhar (1949).
- I : total intensity. For linear polarization :

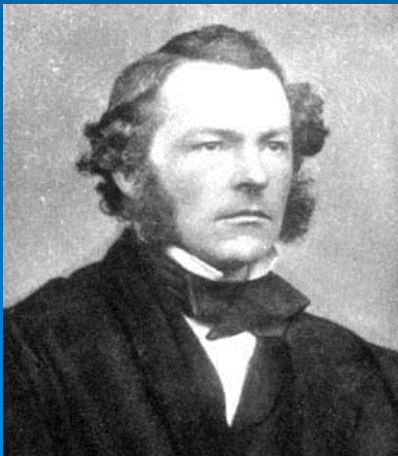
$$V = 0$$

$$Q = I PF \cos(2PA)$$

$$U = I PF \sin(2PA)$$

$$PF = \frac{\sqrt{Q^2 + U^2}}{I}$$

$$PA = \frac{1}{2} \text{Arctg} \left(\frac{U}{Q} \right)$$





Probability law

We use the following probability law, which take into account that PA and PF are not independent, and based on gaussian distributions for the orthogonal Stokes components:

$$dP(a, \psi) = \frac{N_{pt} S^2}{\pi \sigma_S^2} \exp\left[-\frac{N_{pt} S^2}{2 \sigma_S^2} [a^2 + a_0^2 - 2aa_0 \cos(2\psi - 2\psi_0)]\right] a da d\psi$$

$$N(\psi) = S[1 + a_0 \cos(2\psi - 2\psi_0)]$$

Errors on one parameter are given by integrating this law
over the other parameter

The IBIS/Compton mode data analysis

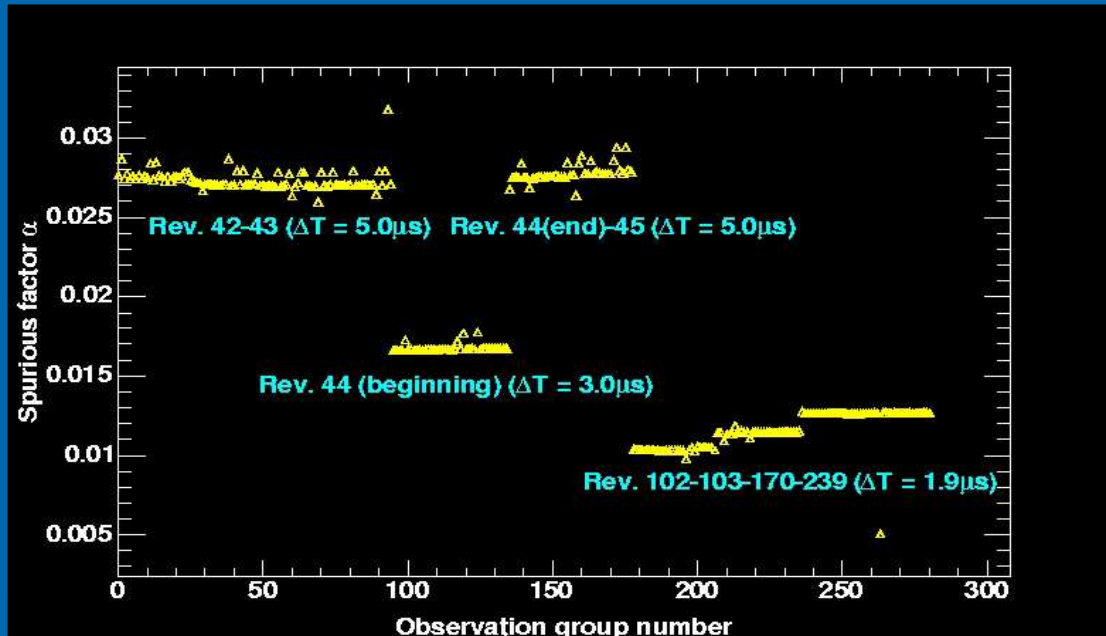


Data analysis summary

- Event selection (energy, pulsar phase)
- Spurious events correction
- Uniformity correction
- Coded mask deconvolution



Spurious correction



“SPURIOUS EVENTS”



1 ISGRI event + 1
independent PICSIT event
detected during the
coincidence window

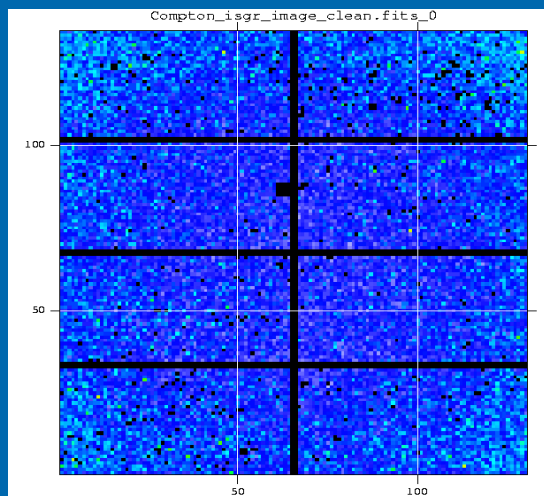


False source detection

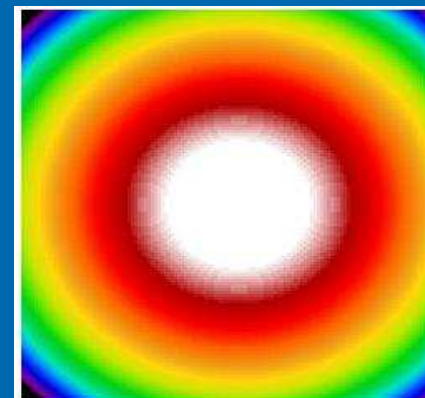
1. We compute the spurious events contribution: $N_{SPUR}/N_{ISGRI} \sim \tau_w N_{PICSIT}$
2. We compute “fake” spurious events, composed of one ISGRI single event randomly associated to one PiCsIT single event.
3. We build sky image with these events that we subtract from the Compton ones.



Compton imaging: Non-uniformity corrections

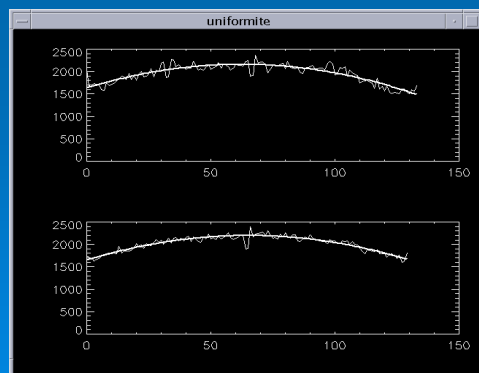
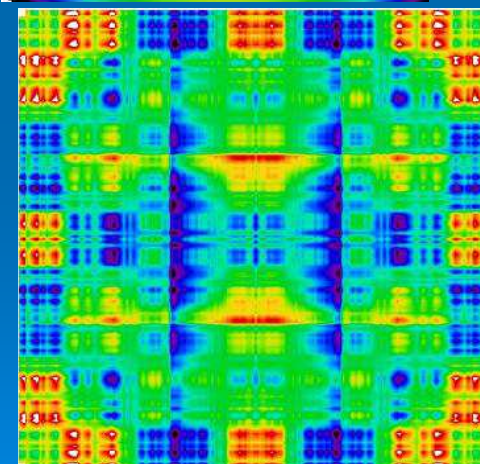


Compton/ISGRI
image



Uniformity map

Uniformity map
deconvolved

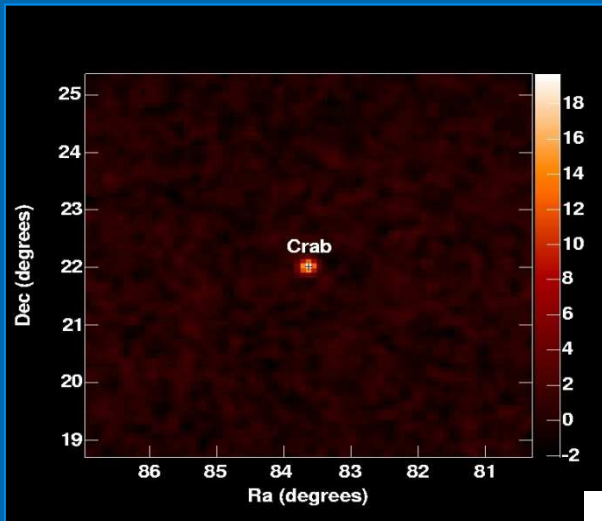


Uniformity profiles

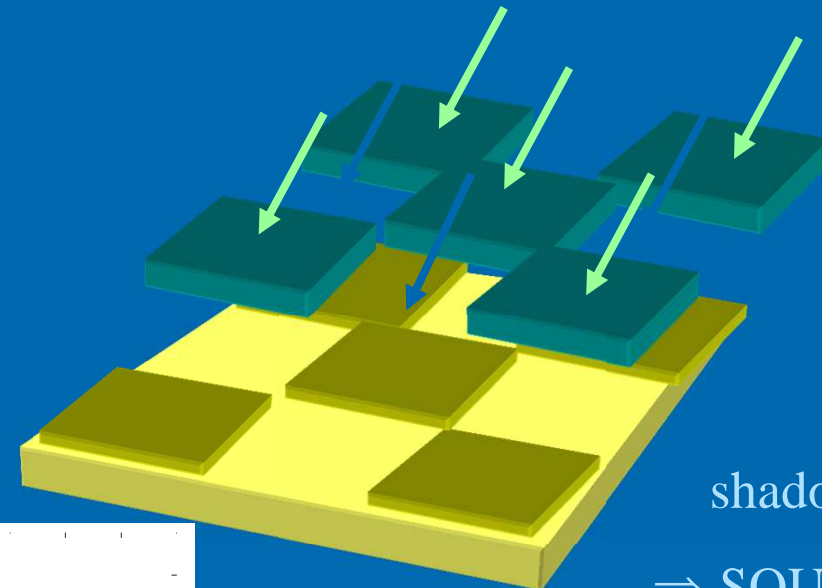


Image deconvolution

200-800 keV T=300 ks

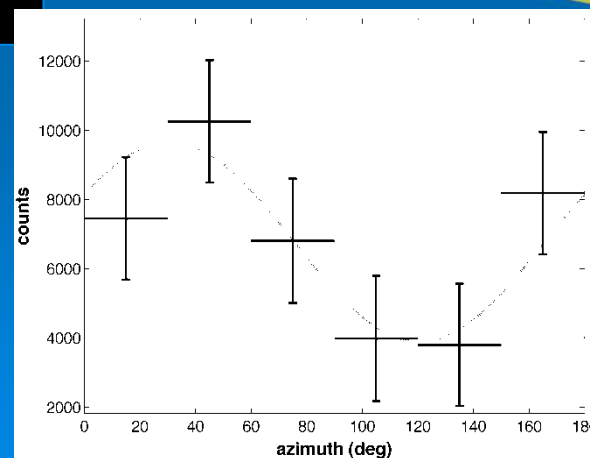


Shadowgram deconvolution



shadow

⇒ SOURCE DIRECTION



maximum modulation for unpolarized data?
(square detectors, grids, pixels, mask pattern...)

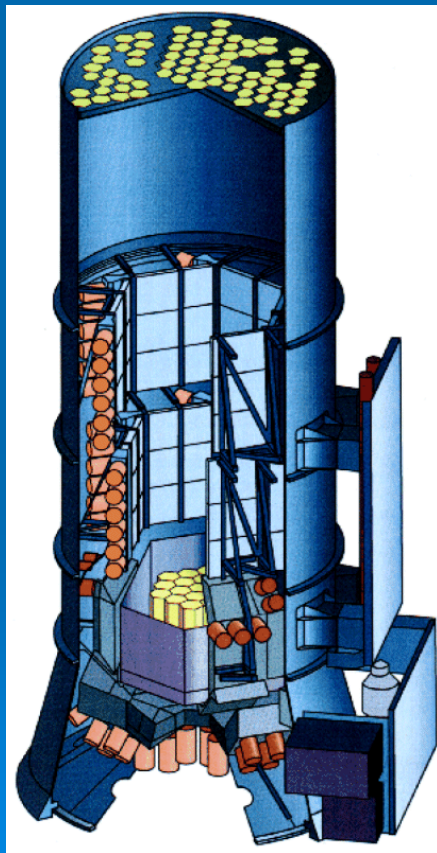
Spurious events

Polarimetry with the SPI telescope

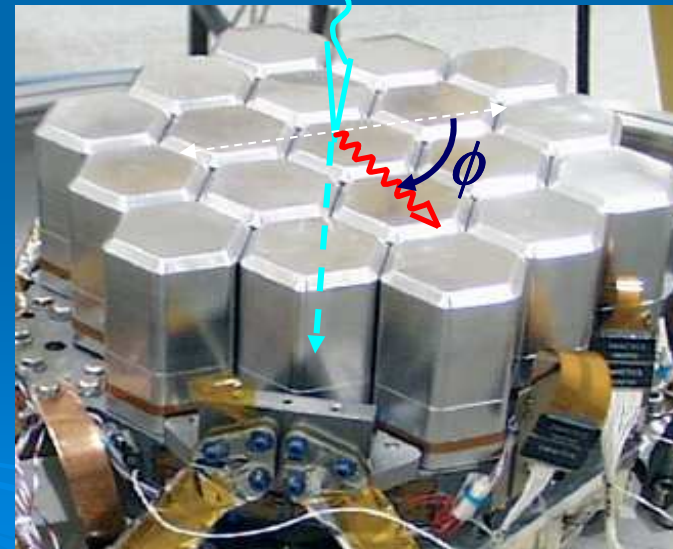


Polarimetry with SPI

SPI can also be used as a Compton telescope using multiple events in the Germanium detectors

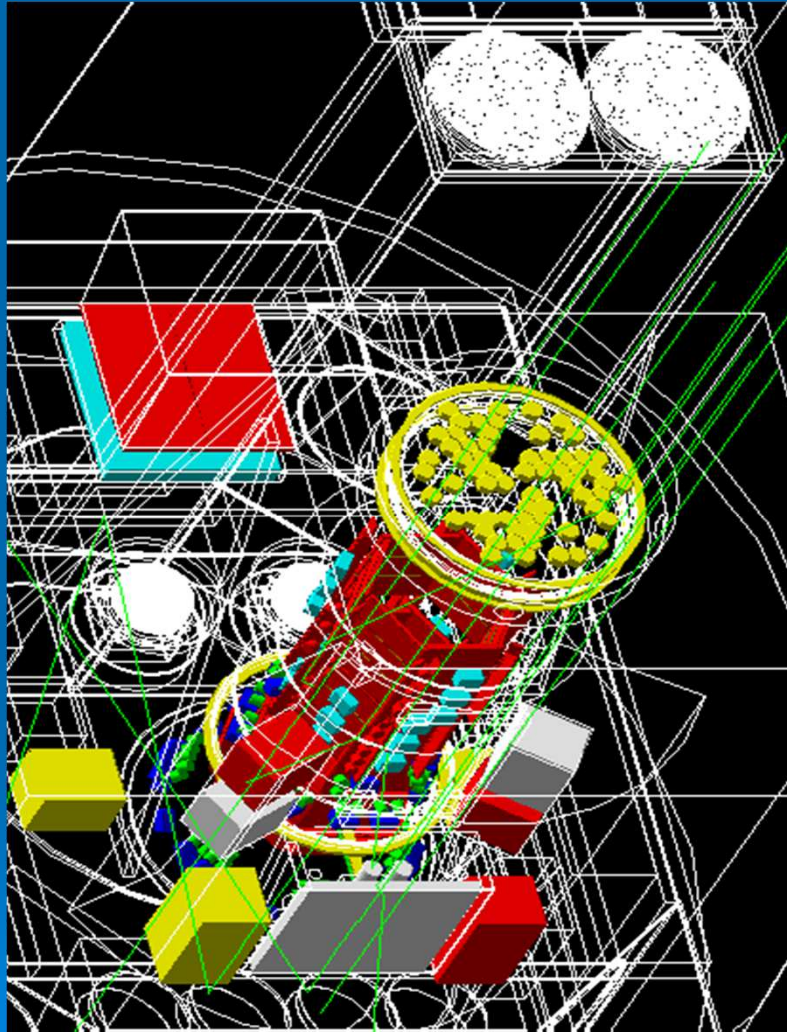


ϕ - angle between incident photon polarisation direction and scattered photon direction.





Polarimetry with SPI



Polarimetry with SPI is determined using a very detailed Mass Model (Dean 08, Chauvin et al. 12)

- *Photons with the same spectrum and direction as the source under investigation are simulated interacting with a detailed model of SPI and the surrounding spacecraft.*
- *The energy deposits can be analysed in the same manner as for the real instrument*
- *The flux is modelled with different angles of polarisation*
- *Then compared to the real data taken by the instrument.*



Polarimetry with SPI (example of the Crab pulsar)

- Mass Model simulation of Crab spectrum for each pointing
- 18 polarised beams for each azimuthal angle in 10° steps between 0° and 170° (180° symmetry) + 1 non-polarised
- $\sim 700,000$ singles & $\sim 70,000$ doubles produced for each pointing
- Polarised & unpolarised simulated data combined to produce any percentage polarisation (Π) needed using:

$$P_{\%} = \frac{\Pi P_{100}}{100} + \frac{(100 - \Pi)}{100}$$

P_{100} = 100% polarised
 P_0 = unpolarised
 $P\%$ = percentage polarised data

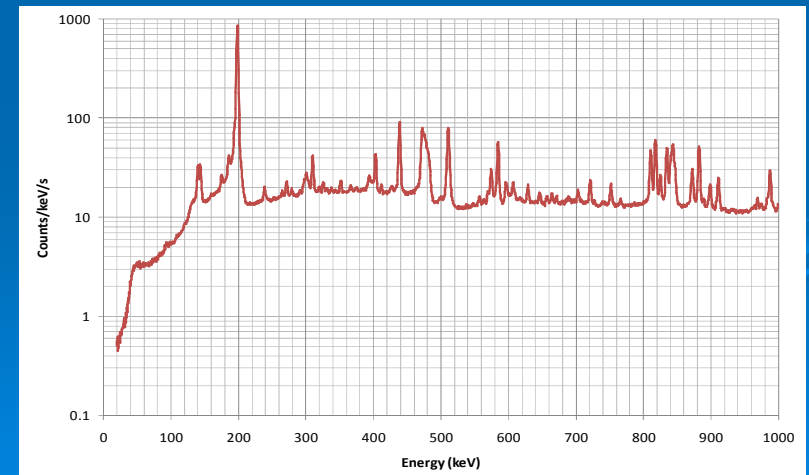


Polarimetry with SPI (example of the Crab pulsar)

- *Data fitted on a Science window by Science window basis*
- *Each adjacent detector pairs considered (Pseudo detectors: 42 later reduced to 32 after failure of the two Ge pixels)*
- *Recorded data from Crab modelled as:*

$$F_{is} = S \times C_{is}(\%, \Pi) + B_s \times B_i$$

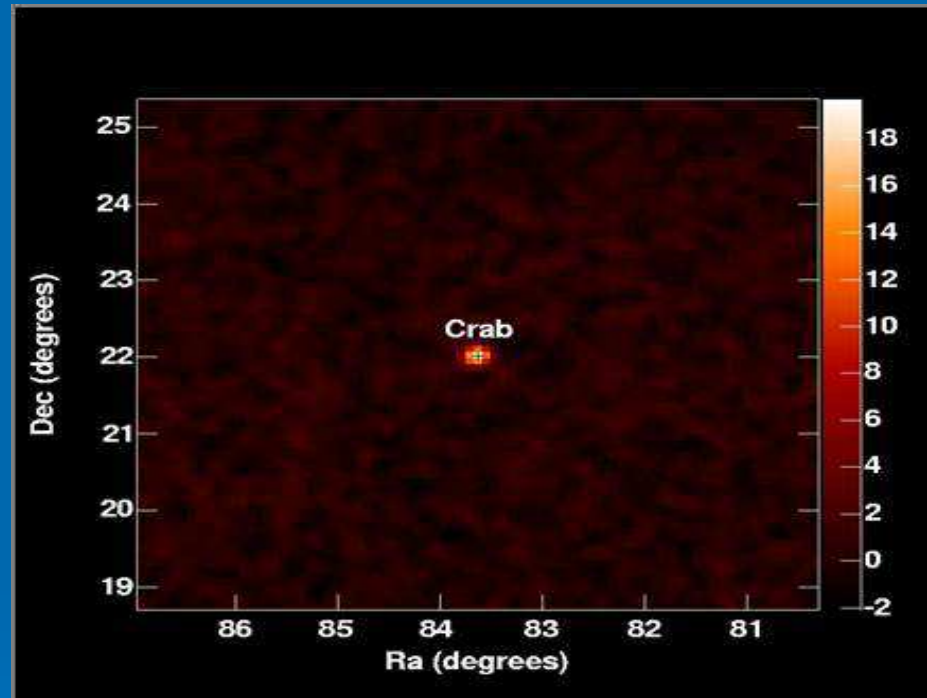
- S = the Crab strength
- C = count distribution from the simulation
- B_i = spatial distribution of the background
- B_s = background variation in time



The Crab polarisation between 200 and 800 keV



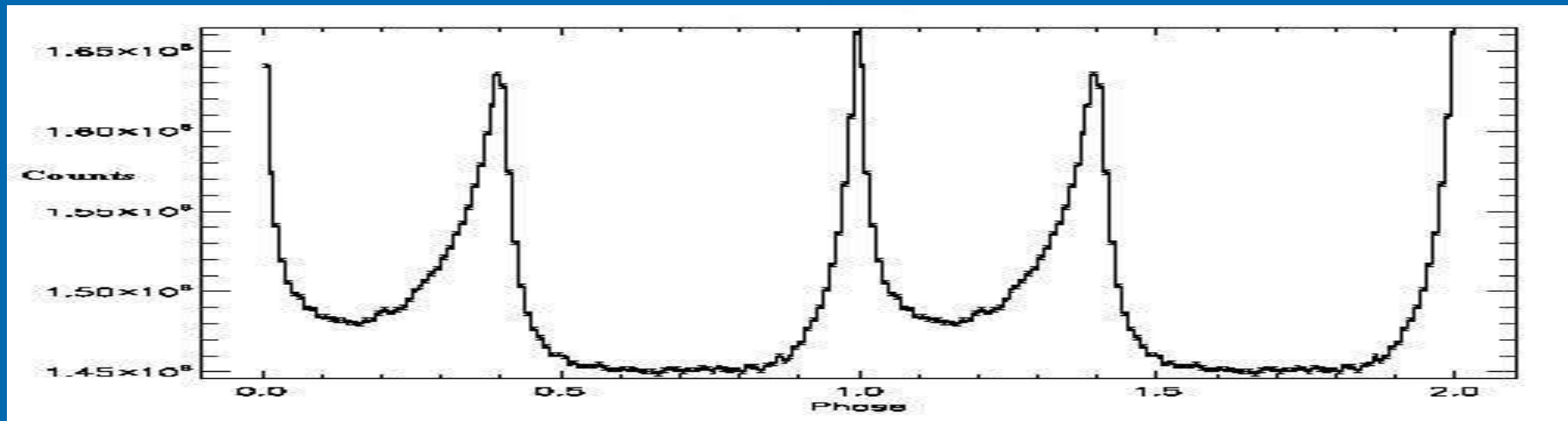
Crab IBIS observations: Imaging



Deconvolved significance map of Crab pulsar using Compton mode, 200-800 Kev, 1 Ms.



Crab IBIS observations: timing



INTEGRAL/ISGRI lightcurve of the Crab pulsar
20-120 keV, 300 ks, 100 bins.



Crab observations log

Forot et al. 2008 :

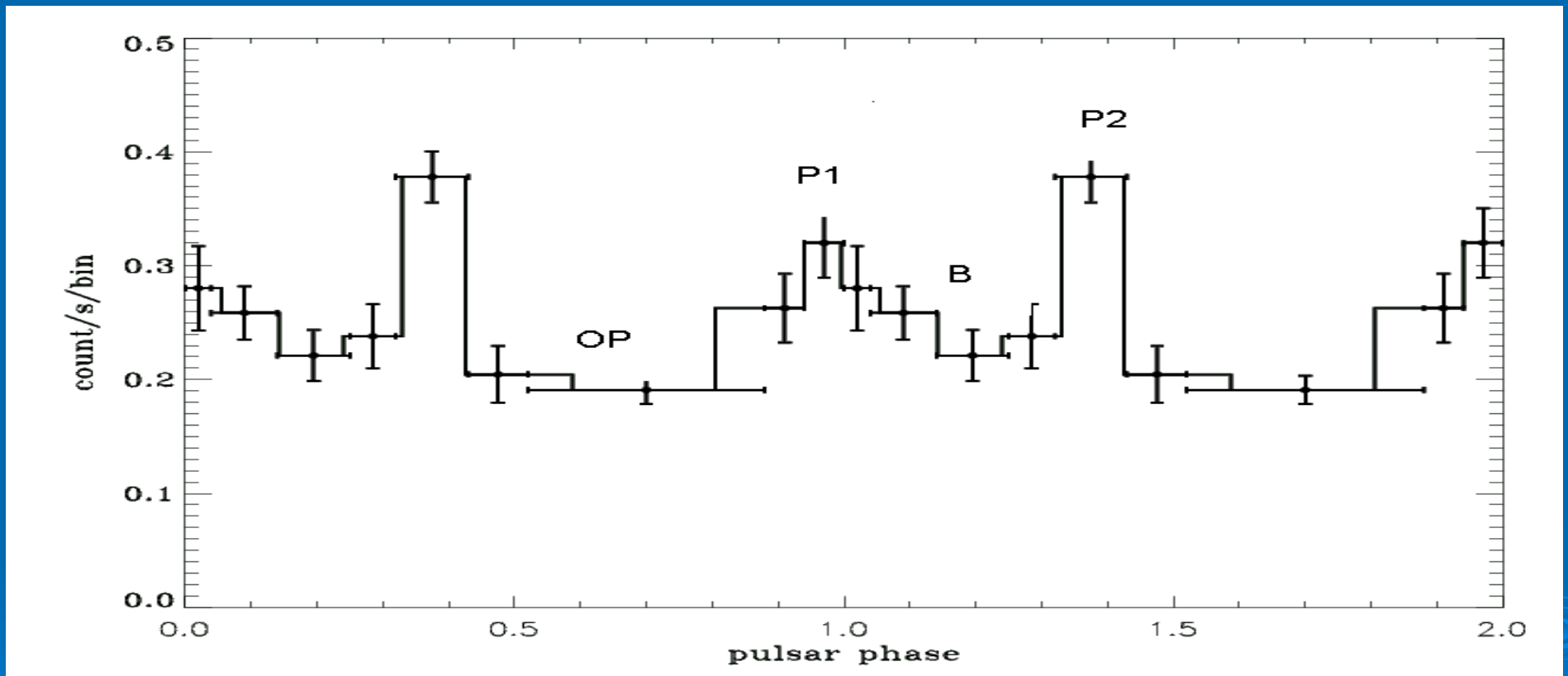
- We observed the Crab nebula from 2003 to 2007 for a total of 1.2 Ms.
- We used Jodrell Bank ephemeris for the pulsar phase computation, and divided data in 4 phase bands.
- We made the analysis in 6 bins in φ azimuth ($0^\circ \leq \varphi \leq \pi$).

P_1	$0.88 < \Phi < 0.14$
B	$0.14 < \Phi < 0.25$
P_2	$0.25 < \Phi < 0.52$
OP	$0.52 < \Phi < 0.88$

Phases
according to
Kuiper et al.
'01



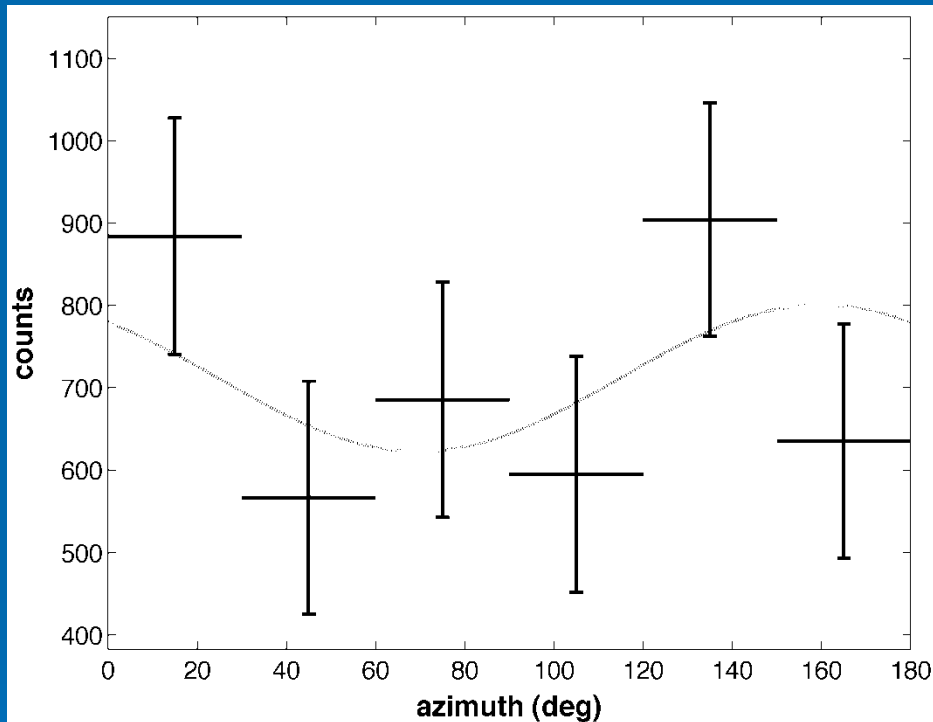
Crab Compton mode light curve



Compton Mode lightcurve of Crab pulsar, 200-600 Kev, 2.6 Ms.

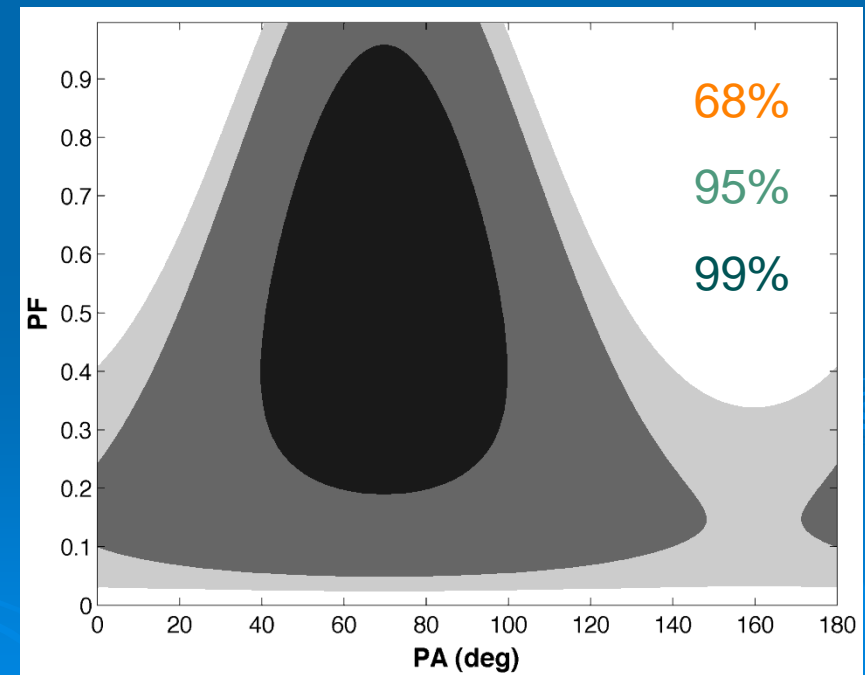


azimuth profile: P1+P2 peaks



$$PA = 70.0^\circ \pm 20.0^\circ$$

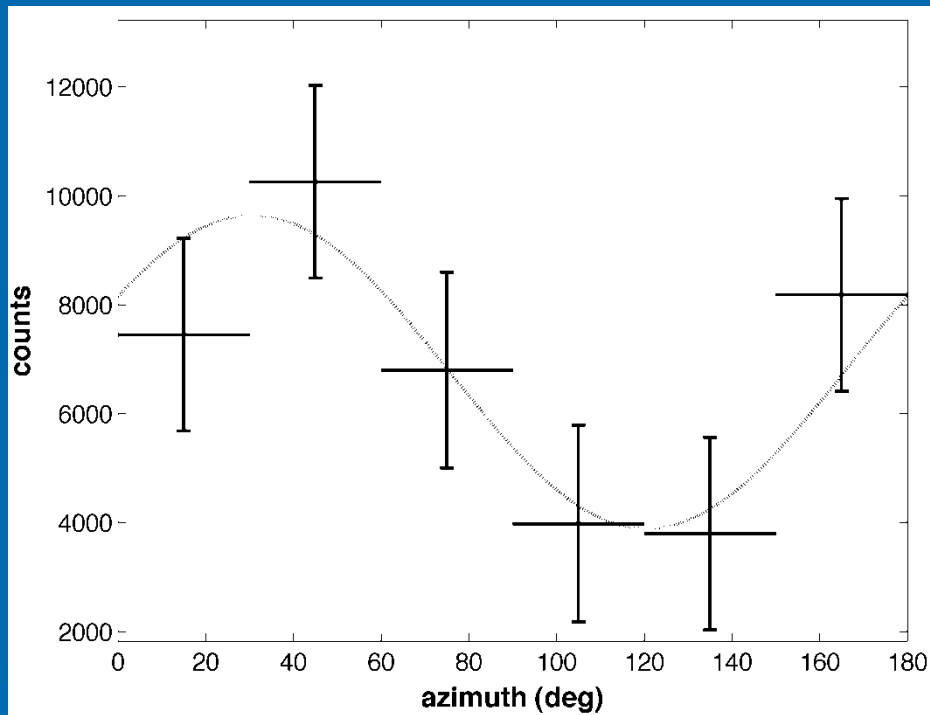
$$PF = 0.42 \pm {}^{0.30}_{0.16}$$



$$\text{proba}(a > a_0, \text{ any } \varphi) = 33.5 \%$$

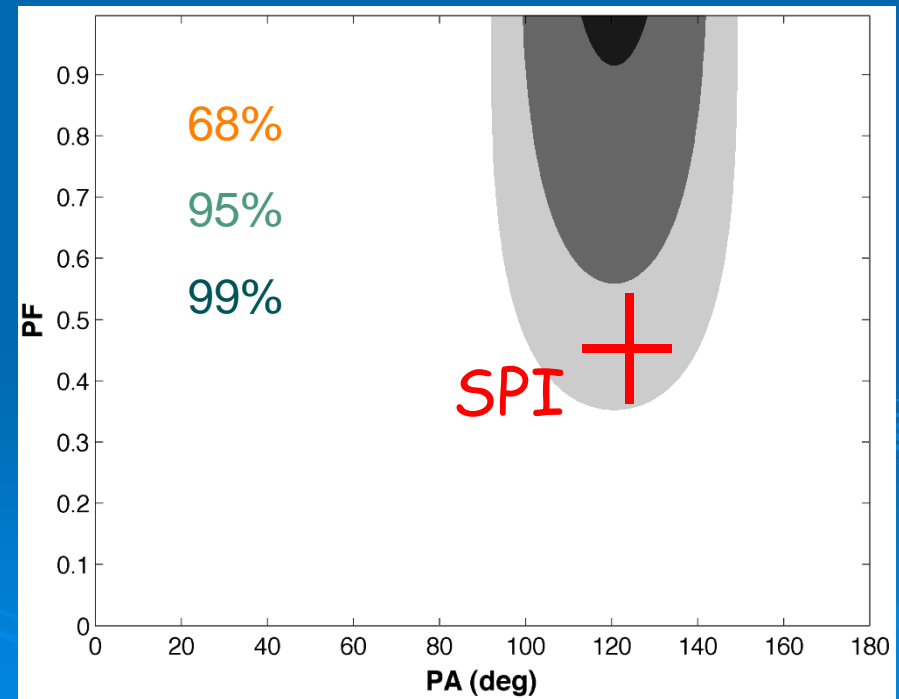


azimuth profile: off-pulse



$$PA = 120.6^\circ \pm 8.5^\circ$$

$$PF > 0.72$$

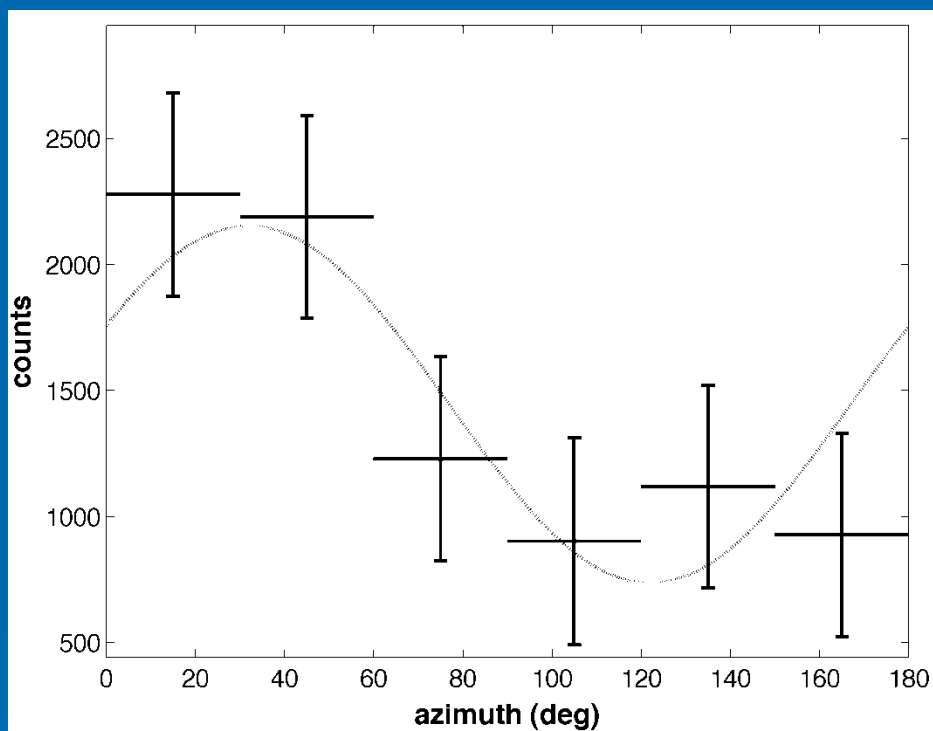


$$\text{proba}(a > a_0, \text{ any } \varphi) = 0.26 \%$$

SPI : $PA = 123^\circ \pm 11^\circ$
 $PF = 46 \pm 10 \%$
(Dean et al., 2008)

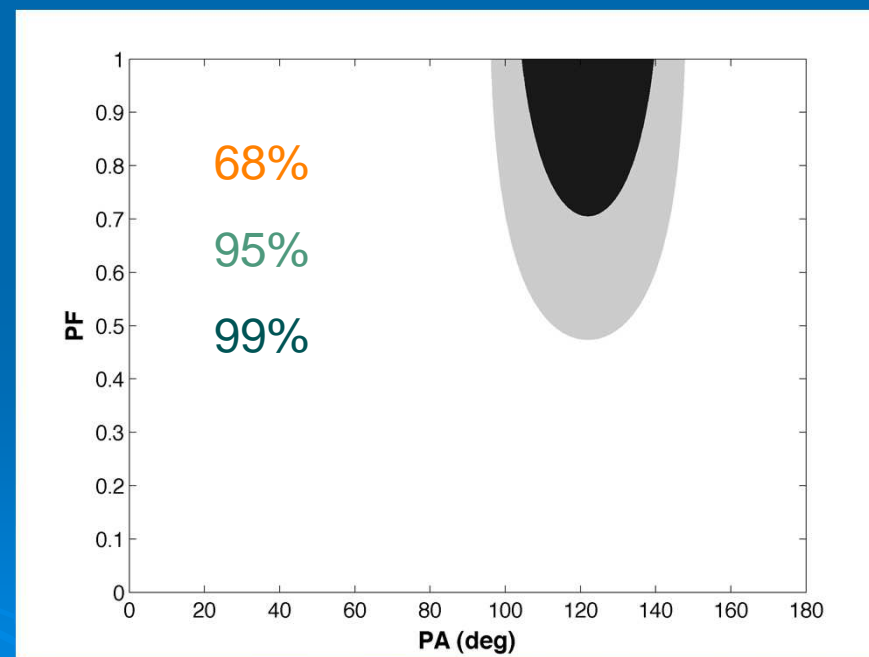


azimuth profile: off-pulse + bridge



$$PA = 122.0^\circ \pm 7.7^\circ$$

$$PF > 0.88$$



$$\text{proba}(a > a_0, \text{ any } \varphi) = 0.10 \%$$



OP polarization // rotation axis

polarization angles

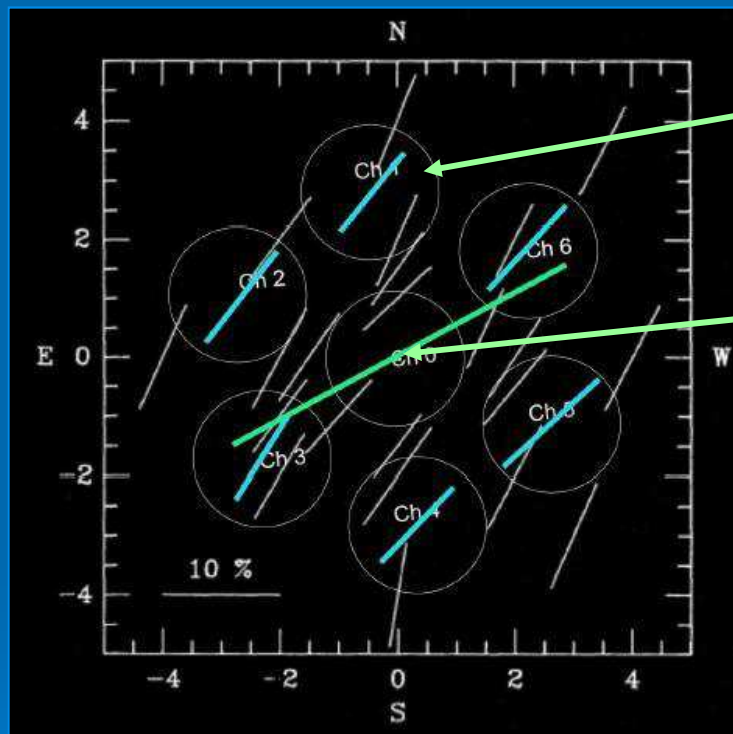
off-pulse: $PA = 120.6^\circ \pm 8.5^\circ$

projected rotation axis:

$124.0^\circ \pm 0.1^\circ$

optical $r < 0.01$ pc: $PA = 119^\circ$

X-ray: $PA = 152^\circ$



152°

8%

119°

33%

Slowikowska et al. 06

Smith et al. '88

Weisskopf et al. '78



Summary and comparison with the SPI results

OP $PA = 120.6^\circ \pm 8.5^\circ$
 $PF > 0.72$

OP + B $PA = 122.0^\circ \pm 7.7^\circ$
 $PF > 0.88$

$P_1 + P_2$ $PA = 70.0^\circ \pm 20.0^\circ$
 $PF = 0.42 \pm \begin{matrix} 0.30 \\ 0.16 \end{matrix}$

SPI +

Polarisation of Cygnus X-1 at MeV energies

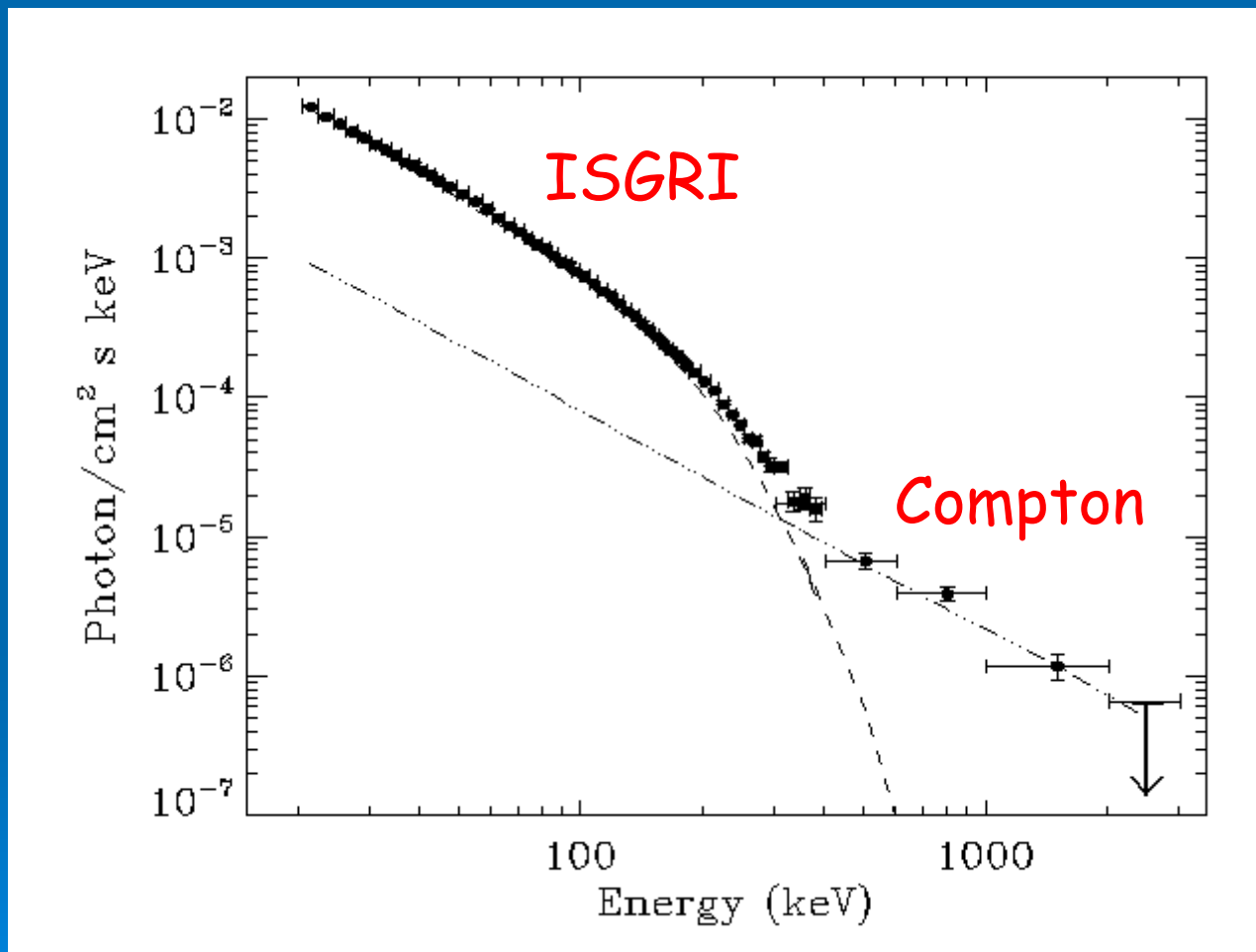


Cygnus X-1 observations log

- We have observed Cygnus X-1 from 2003 to 2009 for a total of 5 Ms.
- We have summed all IBIS data over Cygnus X-1 spectral states. A more detailed analysis making selection according to the source states is on-going.
- As usual, we made the analysis in 6 bins in φ azimuth ($0^\circ \leq \varphi \leq \pi$).



Cygnus X-1 high energy spectrum



Two spectral components:

20-400 keV

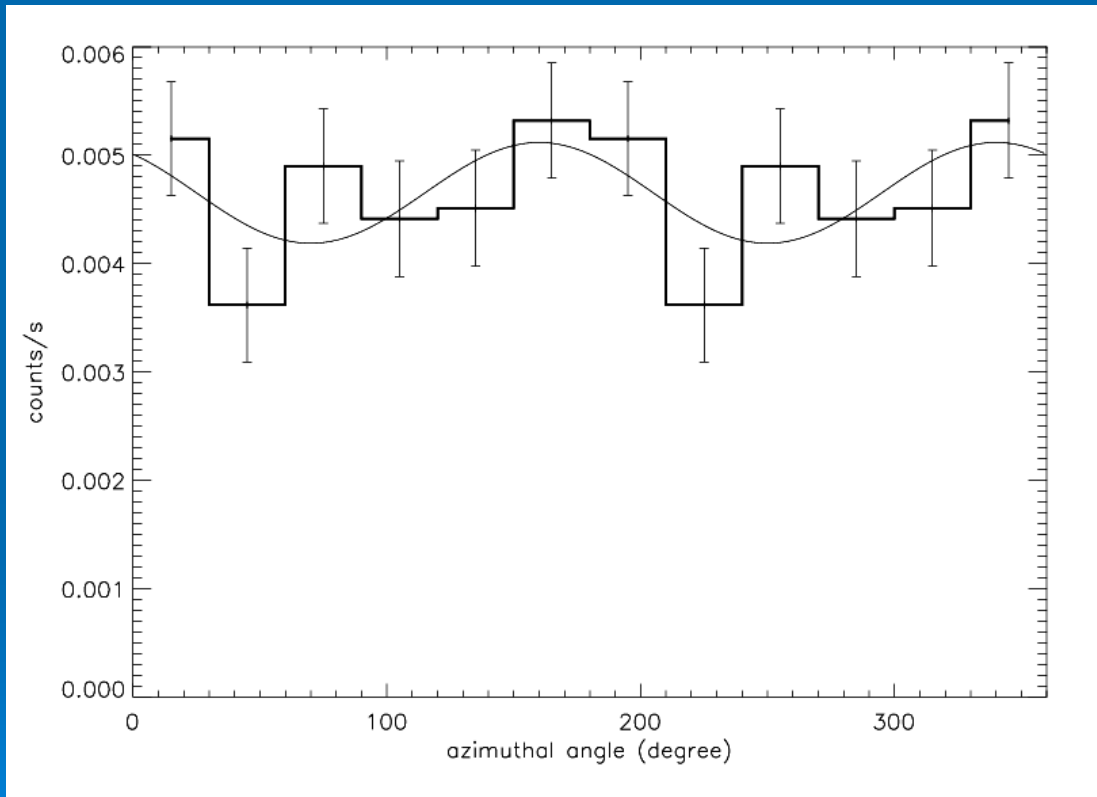
Thermal
Comptonisation

400 -2000 keV

?



Cygnus X-1 polarisation (200-400 keV)

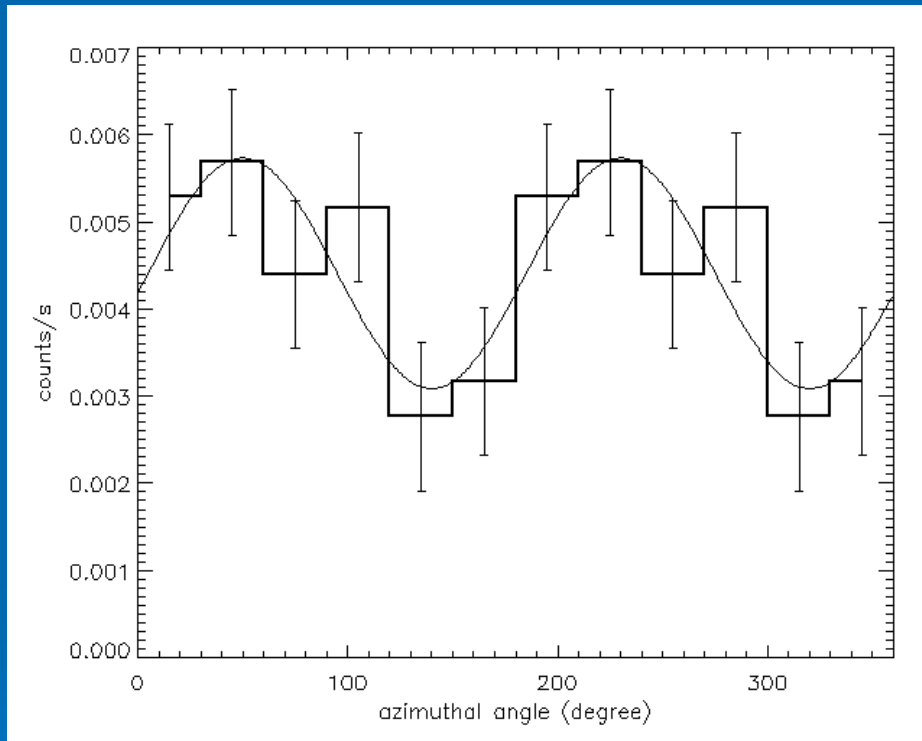


Polarisation
fraction lower
than 20%
(90 % c.l.)

Consistent with
comptonisation



Cygnus X-1 polarisation (400 - 2000 keV)



Polarisation fraction

$67 \pm 30 \%$

(90 % c.l.)

Synchrotron ?

$PA = 40 \pm 8^\circ$

- Polarization signal confirmed by SPI. (Jourdain et al., 2012)
- $\sim 60^\circ$ away from the compact radio jet position (-21° :- 24°).



MeV synchrotron tail ?

Hard tail photon index : $N_{ph}(E) \sim E^{-\Gamma}$

With $\Gamma = 1.6 \pm 0.2$

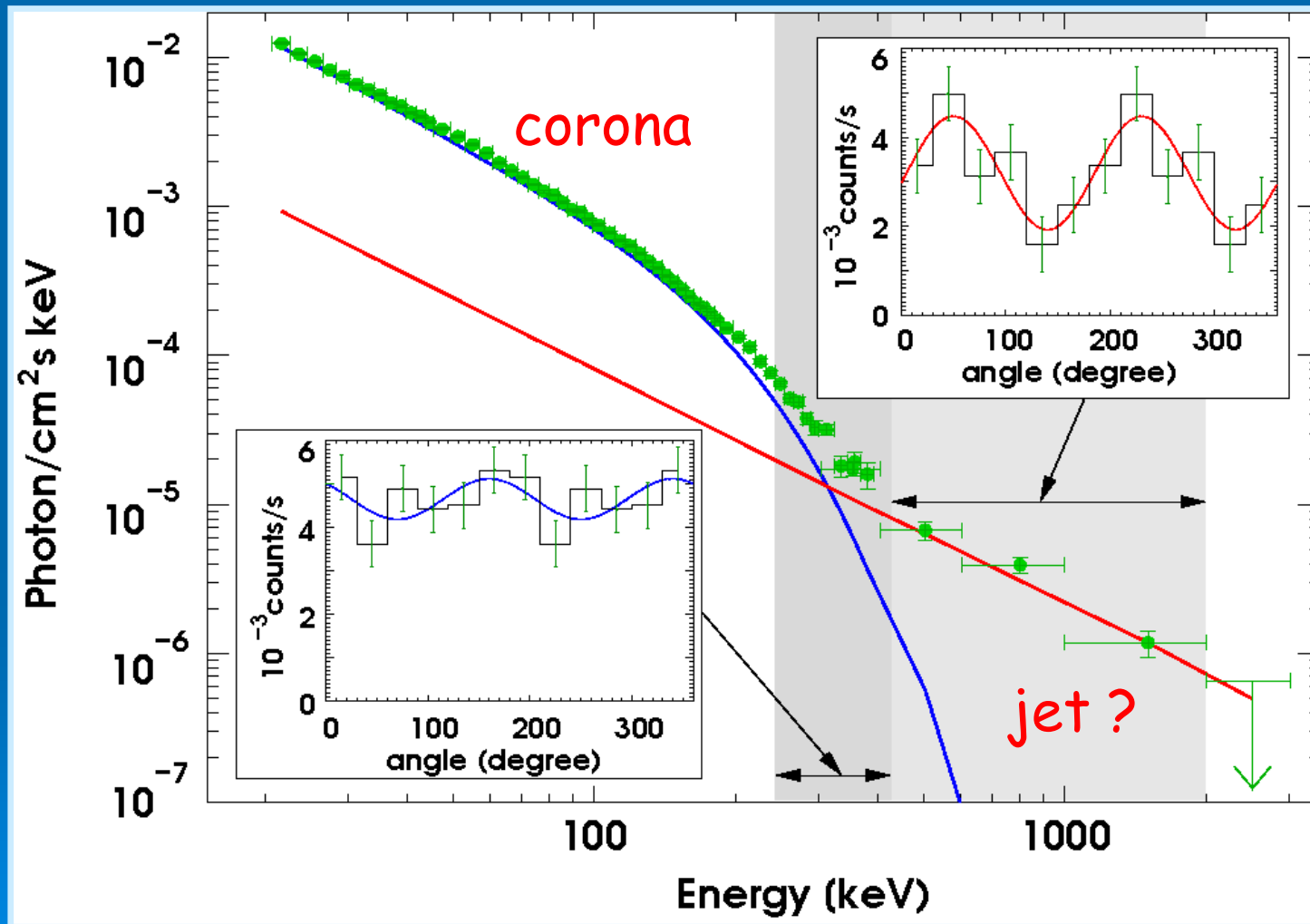
$$\Gamma = -(p-1)/2 \Rightarrow p = -2.2 \pm 0.4$$

Consistent with shock acceleration

If $B = 10$ mG, we need TeV electrons, which have, in these conditions, a synchrotron lifetime of around one month.



Cygnus X-1 summary



INTEGRAL measurements of GRB polarization

November, 7th 2012

History of GRB polarization observations

1. The past : RHESSI
2. The present : INTEGRAL and GAP
3. The future : POLAR, NuStar, Astro-H, ...

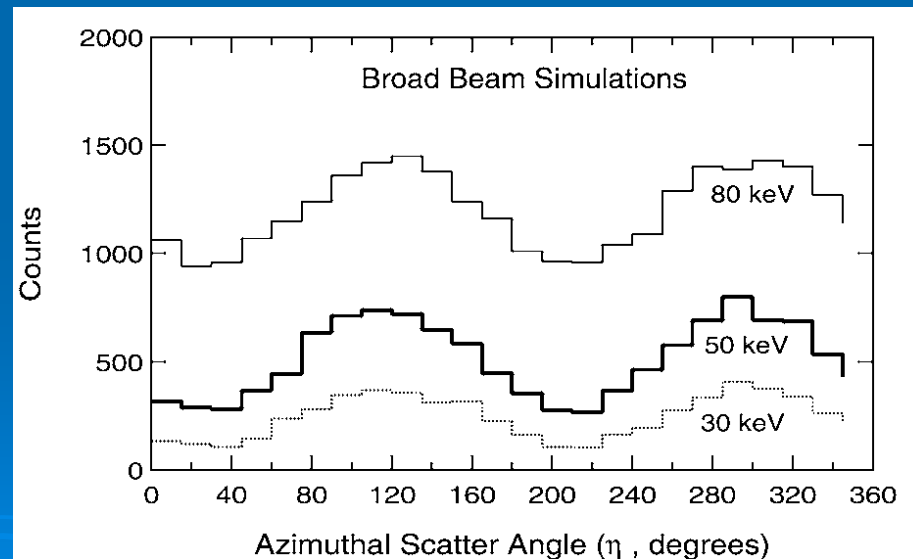
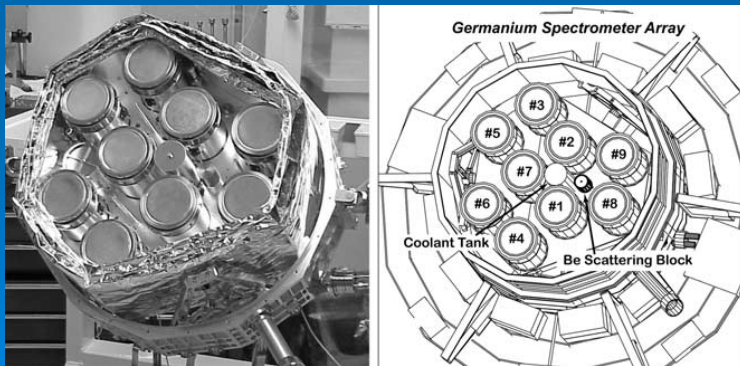
GRB RHESSI observations

1. The RHESSI spectrometer.
2. Observation of polarization in GRB 021206.
3. Controversy on this measure.

The RHESSI spectrometer

- Launched in 2002 to study solar activity.
- 9 germanium detector with modulated coded mask.
- Could measure polarization between 20 and 2 MeV.
- $a_{100} \sim 40\%$ at 50 keV.

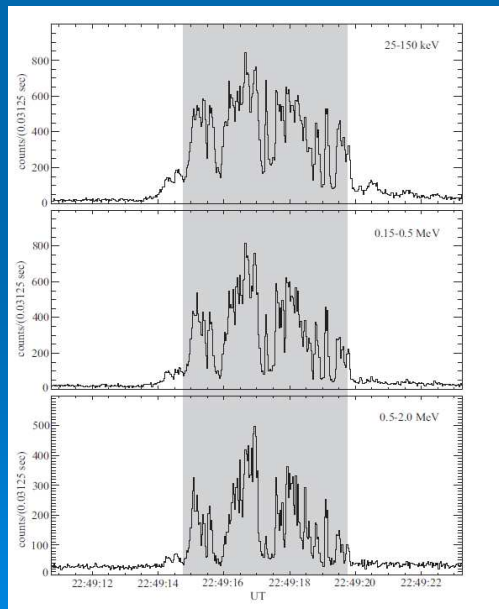
Mc Connell et al.,
2002, Solar Phys. 210, 125



RHESSI observation of GRB021206

GRB 021206 : a bright GRB detected up to 2 MeV.

Data analysis : unpolarized signal simulated by Monte-Carlo and subtracted to real data.

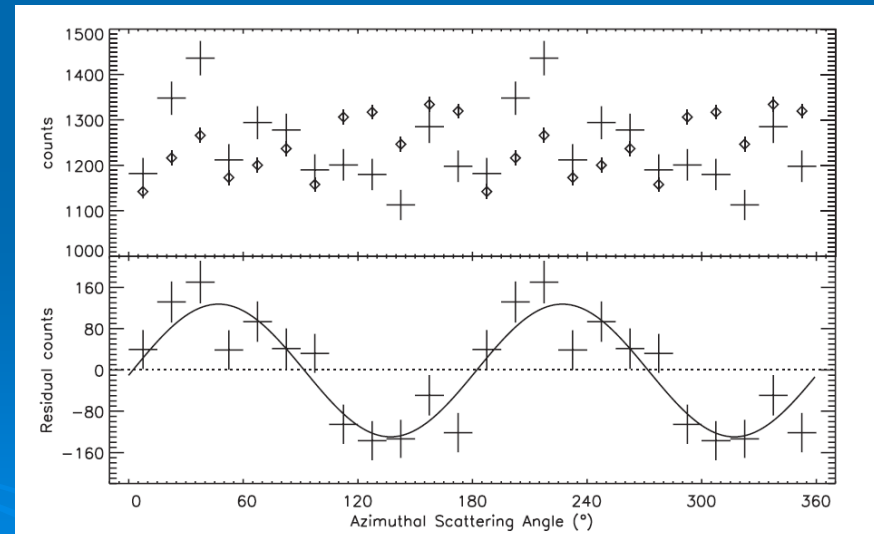


25 - 150 keV

150 - 500 keV

500 keV - 2 MeV

Coburn & Boggs,
Nature, 2003, 423, 415



150 keV - 2 MeV

Controversy

- Data reanalyzed in 2004 by Rutledge & Fox (MNRAS 350, 1288 (2004)) :
 1. Real double events number is a factor 10 below than this estimated by Coburn & Boggs \Rightarrow lower S/N.
 2. Polarization signal is in fact dominated by systematics.

\Rightarrow Difficulty of polarization data analysis

INTEGRAL study of GRB polarisation



GRB 041219A and GRB 061122 in a few words

- GRB 041219A was detected in december 2004 by the Integral Burst Alert System (IBAS). Longest and brightest GRB detected in the Integral FOV so far...
- GRB 061122 was the second brightest burst after GRB 041219A in the Integral FOV, detected in 2006.

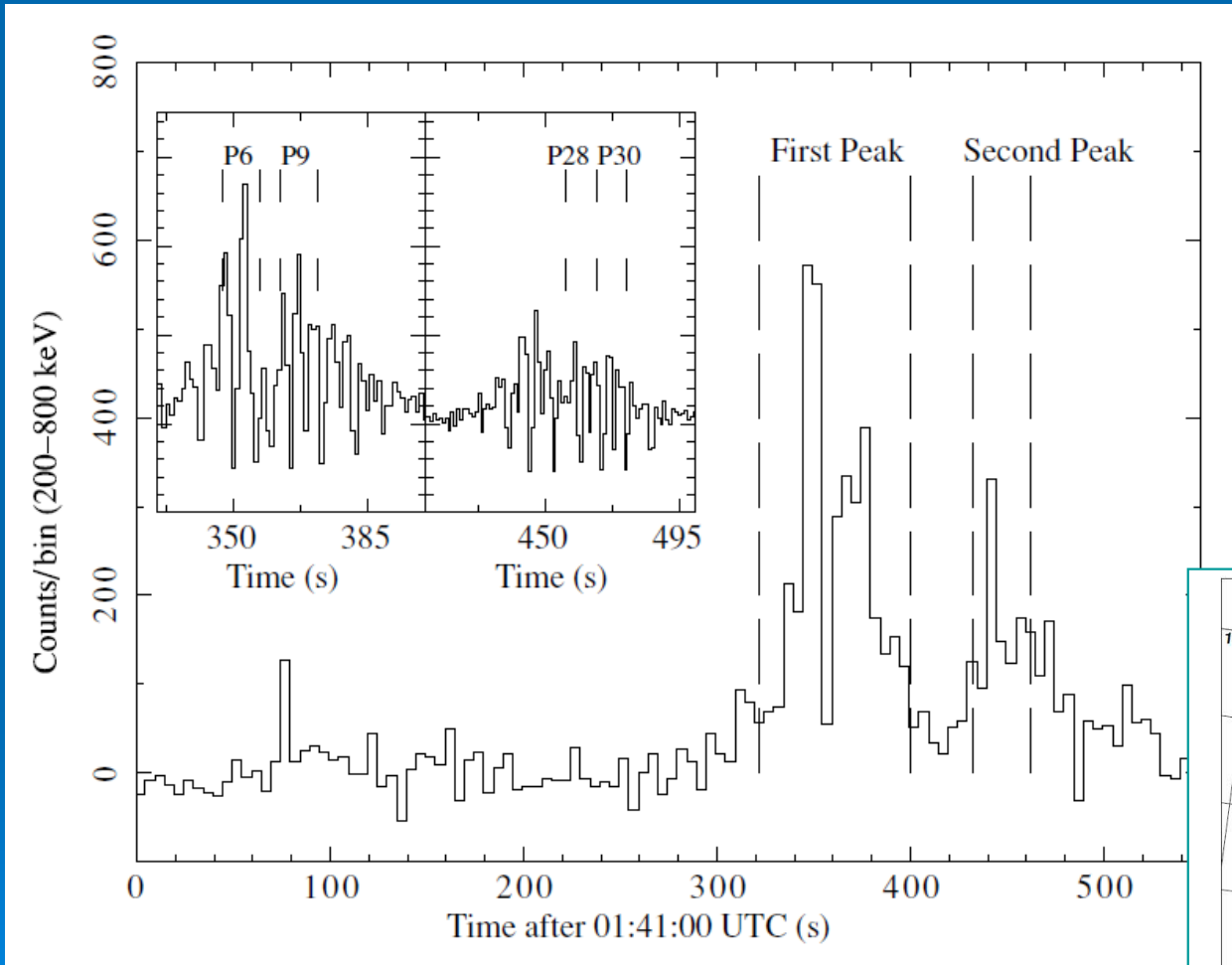


GRB 041219A and GRB 061122 SPI observations

- The Integral Spectrometer (SPI) reported a high polarisation level (68 %) observed during the brightest part of GRB041219A (Mc Glynn et al., 2007).
- An upper limit to the polarization fractions ($< 60\%$) has been computed by Mc Glynn et al. (2009) for GRB 061122.



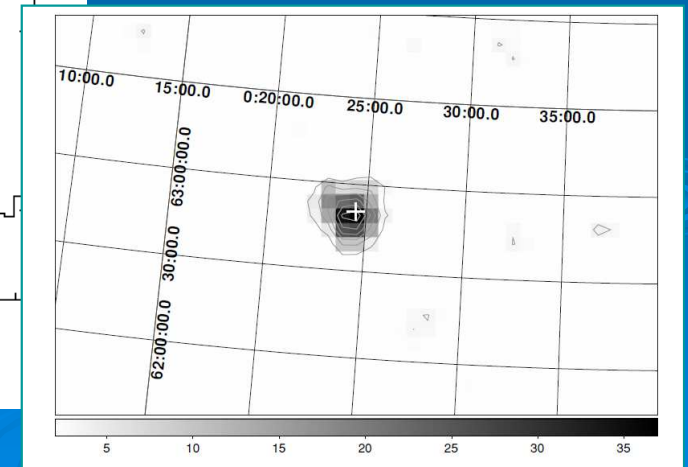
IBIS observation of GRB 041219A: Compton light curve



Analysis in 10s bins

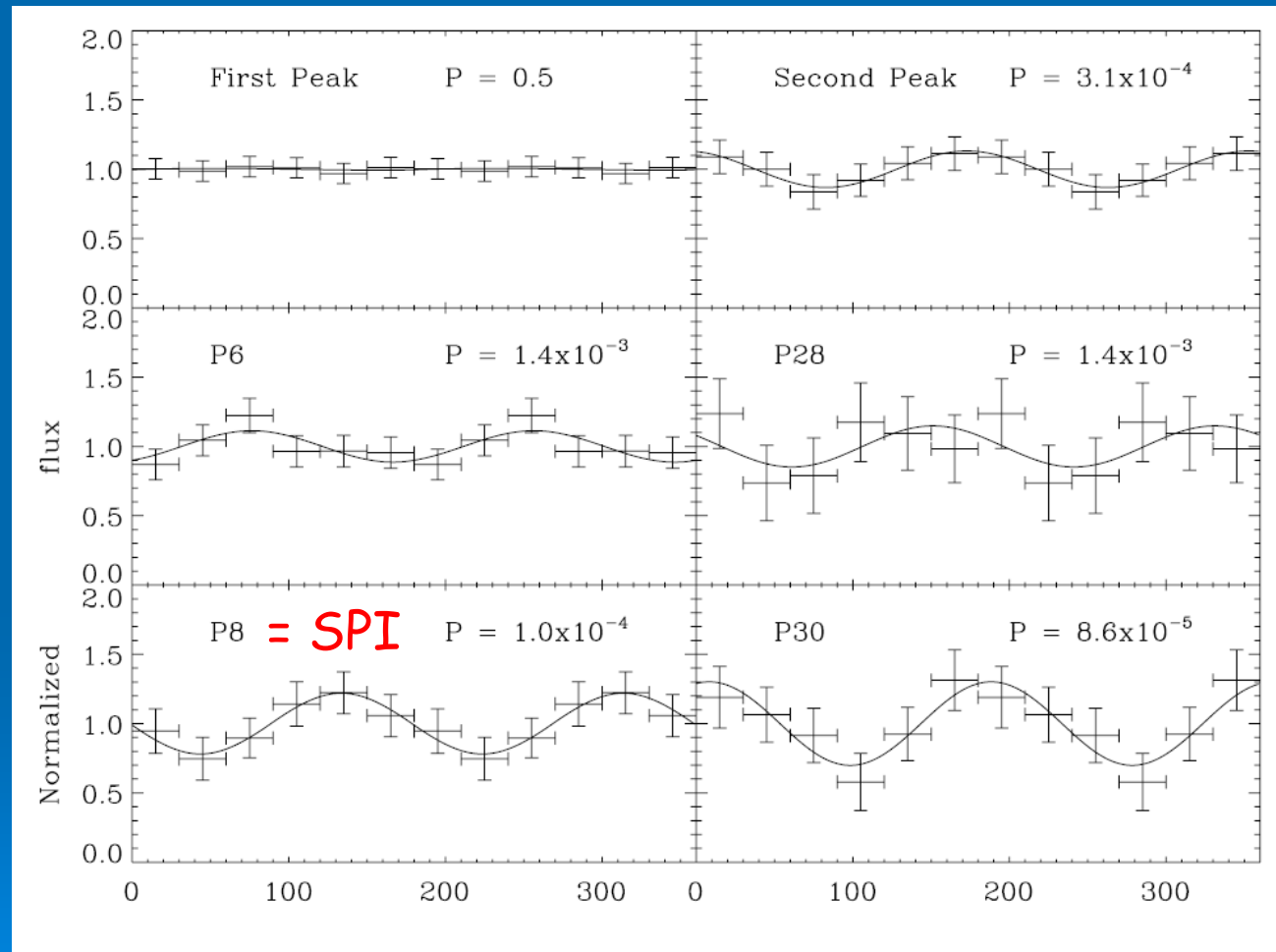
Total S/N
(200-800 keV) :
 37σ

(Götz et al, 2009)





GRB 041219A polarisation diagrams





GRB 041219A polarisation results

Polarization Results for the Different Time Intervals

Name	T_{start} (UT)	T_{stop} (UT)	Π %	P.A. (deg)	Image (SNR)
First peak	01:46:22	01:47:40	<4	...	32.0
Second peak	01:48:12	01:48:52	43 ± 25	38 ± 16	20.0
P6	01:46:47	01:46:57	22 ± 13	121 ± 17	21.5
P8 = SPI	01:46:57	01:27:07	65 ± 26	88 ± 12	15.9
P9	01:47:02	01:47:12	61 ± 25	105 ± 18	18.2
P28	01:48:37	01:48:47	42 ± 42	106 ± 37	9.9
P30	01:48:47	01:48:57	90 ± 36	54 ± 11	11.8

Notes. Errors are given at 1σ c.l. for one parameter of interest.

SPI : 63 ± 30 %

P.A. = $70 \pm 12^\circ$



Interpretation(s)

- (i) synchrotron emission from shock accelerated electrons in a relativistic jet with magnetic field transverse to the jet expansion (Granot 2003, Granot & Königl 2003, Nakar, Piran & Waxman 2003)
- (ii) synchrotron emission from purely electromagnetic flow (Lyutikov et al. 2003, Nakar, Piran & Waxman 2003)
- (iii) synchrotron emission from shock accelerated electrons in a relativistic jet with a random magnetic field (Ghisellini & Lazzati 1999, Waxman 2003)

SAME POLARIZATION LEVELS AS IN (I) BUT A PECULIAR OBSERVATION CONDITION IS NEEDED ($\Theta_{\text{obs}} \cong \Theta_{\text{jet}} + k/\Gamma$)



Interpretation(s)

(iv) Inverse Compton scattering from relativistic electrons in a jet propagating in a photon field ("Compton drag") (Lazzati 2004)

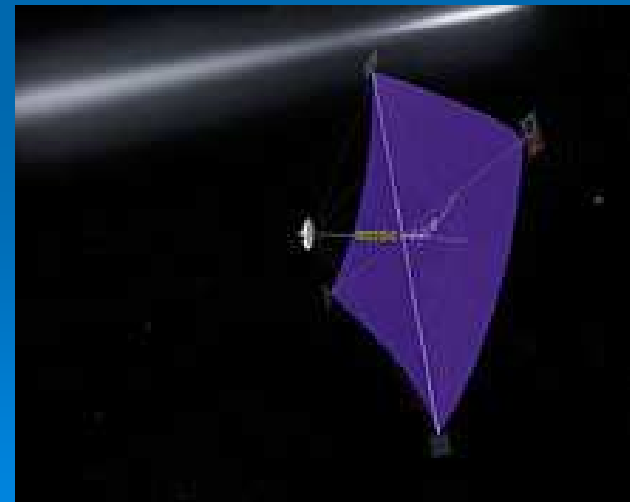
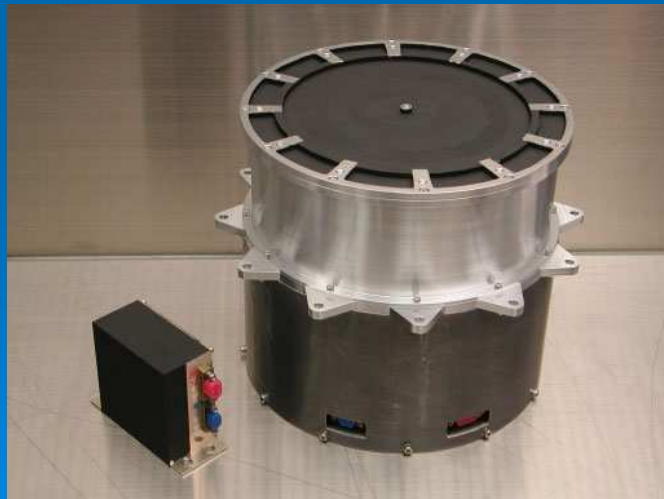
POLARIZATION LEVELS can reach 60-100% BUT ONLY UNDER THE CONDITION OF A NARROW JET ($\Gamma\theta_{jet} < 5$) AND THE SAME OBSERVATION CONDITIONS AS IN (iii) APPLY

(v) Independently from the emission process (synchrotron or inverse Compton), fragmented fireballs (shotguns, cannonballs, sub-jets) can produce highly polarized emission, with a variable P.A. The fragments are responsible for the single pulses and have different Lorentz factors, opening angles and magnetic domains. (e.g. Lazzati & Begelman 2009)

IKAROS/GAP GRB observations

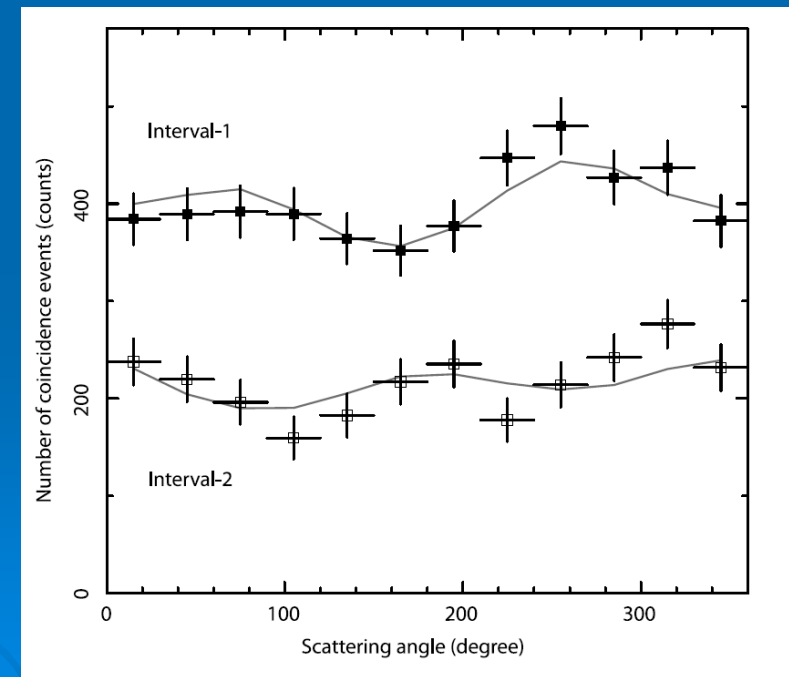
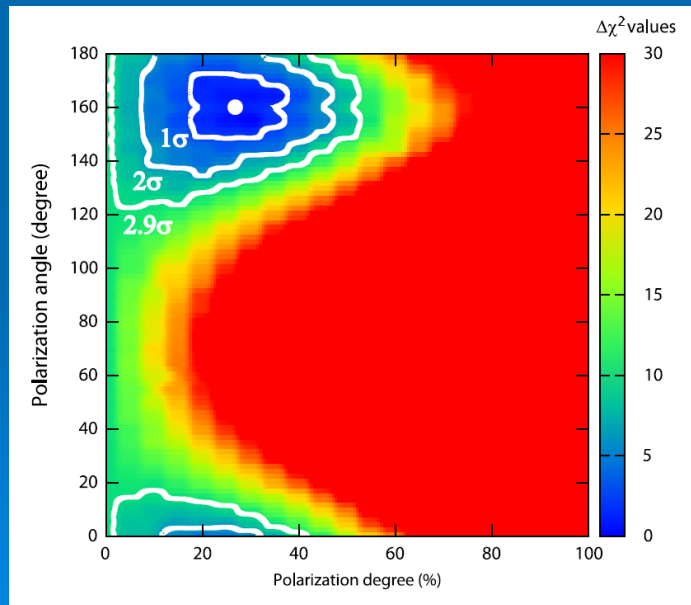
The IKAROS/GAP experiment

- Japanese experiment launched in 2010.
- GAP : Gamma-Ray Burst polarimeter on the solar sail IKAROS.
- Plastic - CsI axial Compton telescope.
- Heavily tested on ground in polarized beams.



GAP observation of GRB 100826A

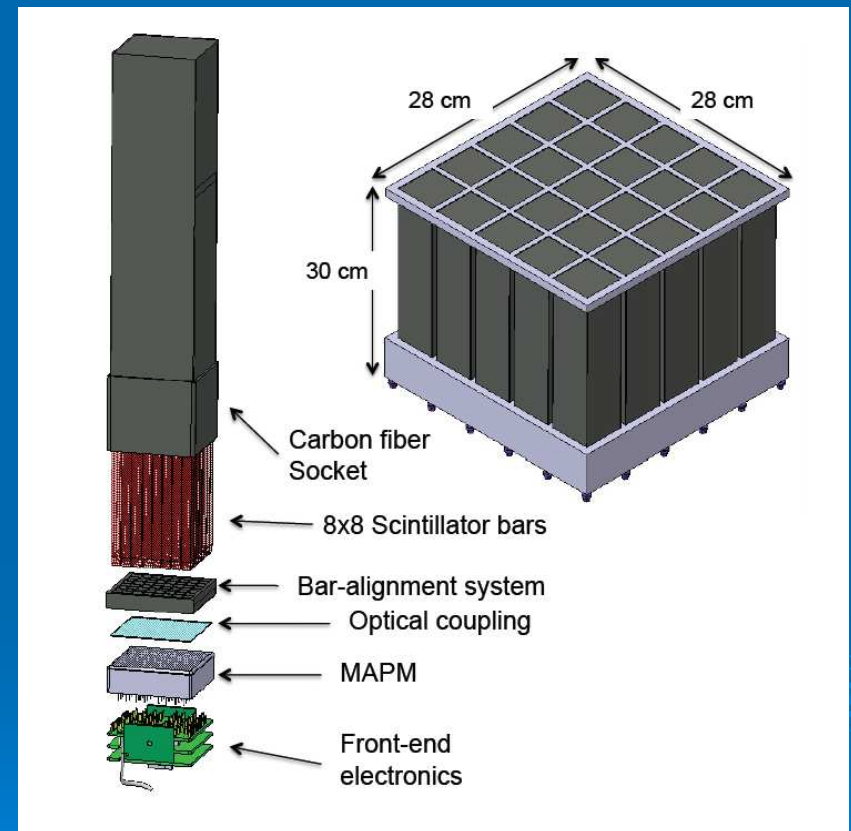
- GRB 100826A observed by GAP (70 - 300 keV).
- Modulation fitted with a Monte-Carlo model.
- Marginal detection at 2.9σ



FUTURE MISSIONS ...

The POLAR telescope (2014)

- POLAR is a Swiss lead mission to be placed on the Chinese space station Tiangong 2 (2014).
- It is a Compton telescope dedicated to GRB polarization measures.
- It consists of several bars of plastic scintillator readout by PMT ($a_{100} \sim 60\%$).

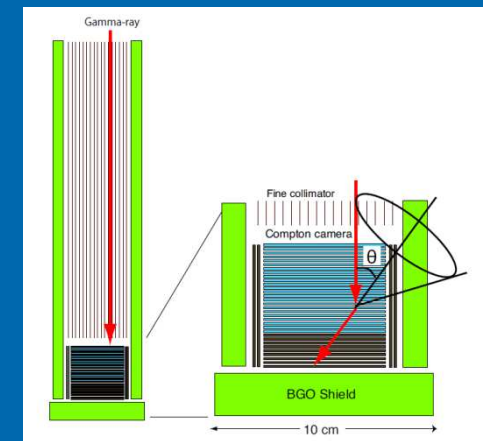
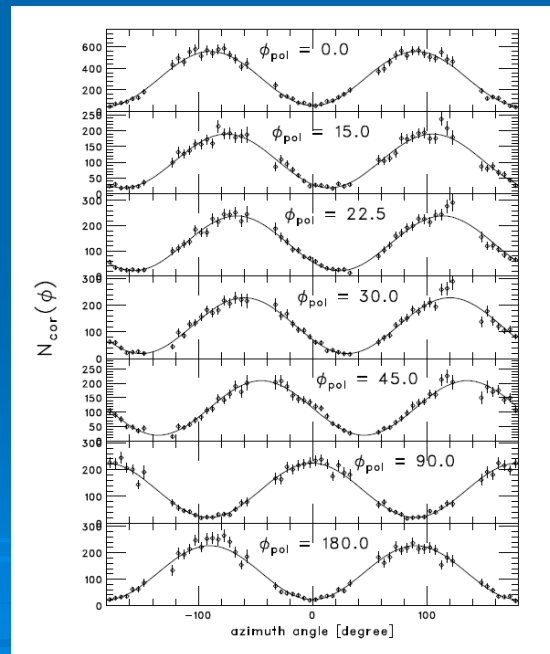


Astro-H (2014)

Astro-H: next X-ray Japanese mission

- 4 instruments including a Compton telescope (SGD, 5-600 keV).
- Good polarimetric results on ground.
- But, FOV (10°), delimited at high energy (> 300 keV) by BGO collimators.

250 keV X-ray beam



SGD telescope

NuStar (2012)

NuStar : new hard X-ray focusing telescope (6-80 keV) launched in June 2012.

- A mirror focuses X-rays toward a CZT detector, 12 m away.
- Polarization measures could be made by studying Compton scatter between different CZT pixels.
- But, small FOV \Rightarrow GRB scarcely observed.



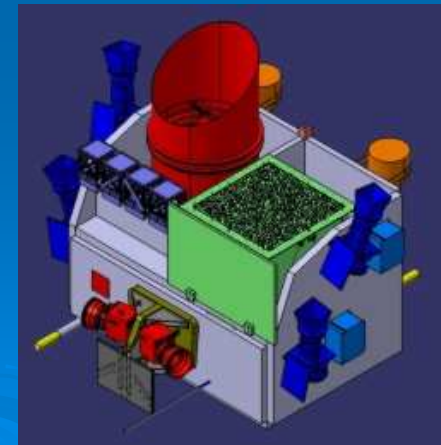
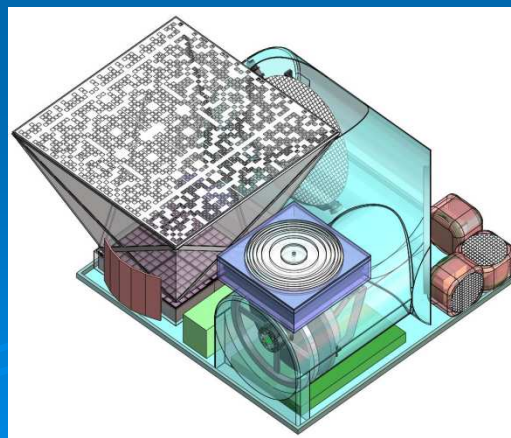
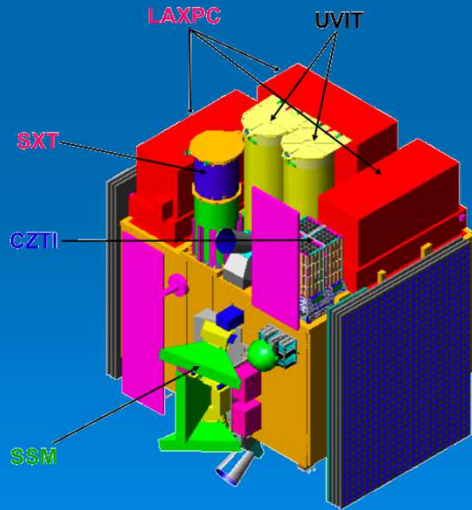
ASTROSAT (2012), UFFO-100 (2015), SVOM (2017), ...

ASTROSAT : next X-ray/UV indian mission

UFFO-100 : russian/korean mission

SVOM : French/Chinese GRB mission

hard X-ray wide field imager: CZT, LSO detector + coded mask
which may be also used as "90° polarimeters".



Conclusion

- The measure of polarization in hard-X/soft-gamma rays is a powerful tool to investigate the emission mechanisms and geometry of Gamma-Ray Bursts.
- Fundamental physics questions can also be addressed
- Next generation polarimeters (e.g., POLAR, Astro-H, etc.) will complement the present discoveries !
- Several Compton telescope R&D projects are on-going all over the world dedicated to hard X-ray polarimetry measurement.

Thank you !



511 keV emission from the Galactic bulge

511 keV line intensity from the bulge : $> 10^{-3}$ photons s^{-1}



Positron injection in the bulge : $> 10^{43}$ e^+ s^{-1}

- Decay of massive particles
- Pair plasma injected by compact sources
- β^+ decay of ^{22}Na from novae
- β^+ decay of ^{56}Co from type Ia supernovae
- β^+ decay of ^{56}Co from hypernovae in the Galactic nucleus
Cassé, Cordier, Paul & Schanne, ApJ 602, L17, 2004
- Annihilation of light dark matter
Boehm, Hooper, Silk, Cassé & Paul, PRL 92, 101301, 2004

- Idea was to write down polarisation state of wave in terms of observables (hard to get hold of varying polarisation ellipse!)
- Observables are intensities averaged over time
- Stokes wrote down his parameters in terms of the intensity passed by some polarizing filters that if illuminated by a randomly polarised wave, transmit half of the incident light.
- Filter 0 passes all states equally, giving intensity I_0
- Filters 1 and 2 pass linearly polarised light at position angles of 0 (horizontal) and 45 degrees, respectively.
- Filter 3 is opaque to left handed circular polarisation

$$I = 2I_0$$

$$Q = 2I_1 - 2I_0$$

$$U = 2I_2 - 2I_0$$

$$V = 2I_3 - 2I_0$$

- I is the total intensity
- Q reflects the tendency for the light to be in a linear state which is horizontal ($Q > 0$), vertical ($Q < 0$) or neither ($Q = 0$)
- U reflects the tendency for the light to be in a linear state at 45 degrees ($U > 0$) or -45 degrees ($U < 0$), or neither ($U = 0$).
- V reflects the tendency for the light to be in a circular state which is right handed ($V > 0$), left handed ($V < 0$) or neither ($V = 0$)



GRB 041219A: constraints on LIV

LIV : Lorentz invariance violation

- LIV => rotation of the polarization angle
- Already studied using the SPI measurement of Crab polarization (Maccione et al. 2008)



GRB 041219A: constraints on LIV

- Principle:

Light dispersion relation:

$$\omega^2 = k^2 \pm \frac{2\xi k^3}{M_{Pl}} \equiv \omega_{\pm}^2 .$$

M_{Pl} : reduced Planck
scale ($2.4 \cdot 10^{18}$ GeV)

$$\omega_{\pm} = |k| \sqrt{1 \pm \frac{2\xi k}{M_{Pl}}} \approx |k| \left(1 \pm \frac{\xi k}{M_{Pl}}\right) .$$



GRB 041219A: constraints on LIV

$$\Delta\theta(p) = \frac{\omega_+(k) - \omega_-(k)}{2} d \approx \xi \frac{k^2 d}{2M_{Pl}}$$

Crab: $\xi < 2 \cdot 10^{-9}$ (Maccione et al. 2008)

GRB : at least 10^5 times further away



GRB 041219A: distance determination

- Redshift measure with the CFHT/WirCAM instrument (Götz et al., 2011):

$$\Rightarrow z = 0.31^{+0.54}_{-0.26}$$

$$\Rightarrow d = [0.222-5.406] \text{ Gpc}$$

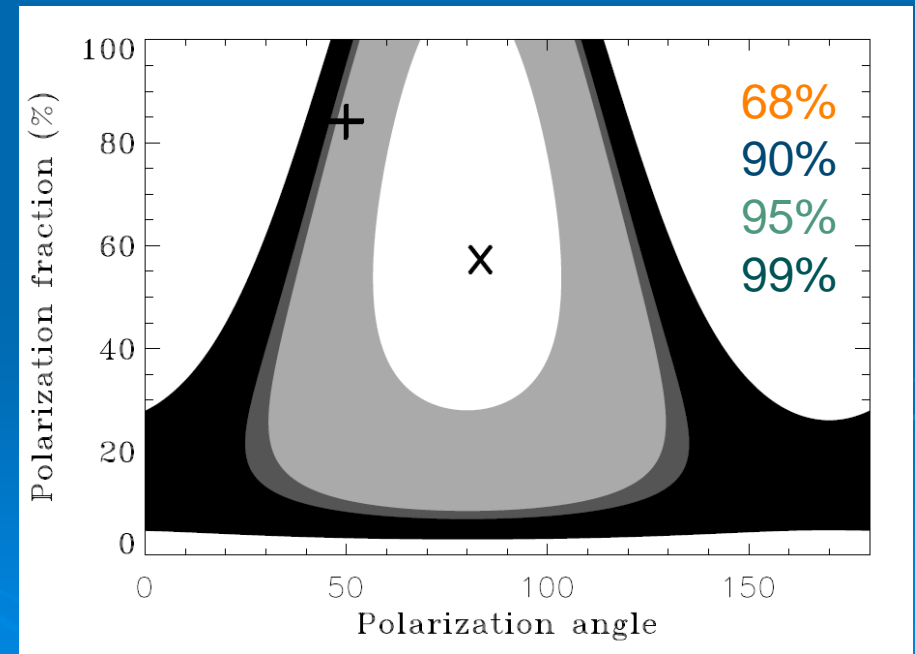
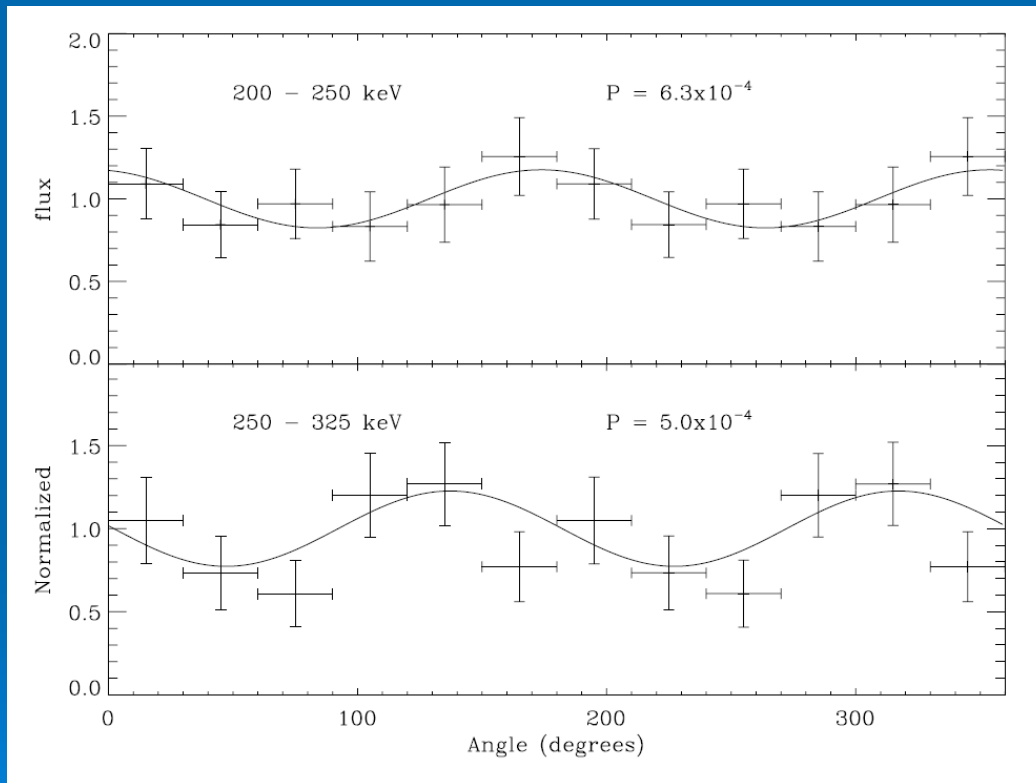
with standard cosmological parameters

$$(\Omega_m=0.3, \Omega_\lambda=0.7, H=70 \text{ km/s/Mpc})$$



GRB 041219A: measure of $\Delta\theta$

Comparison of PA between 2 energy bands with similar signal to noise

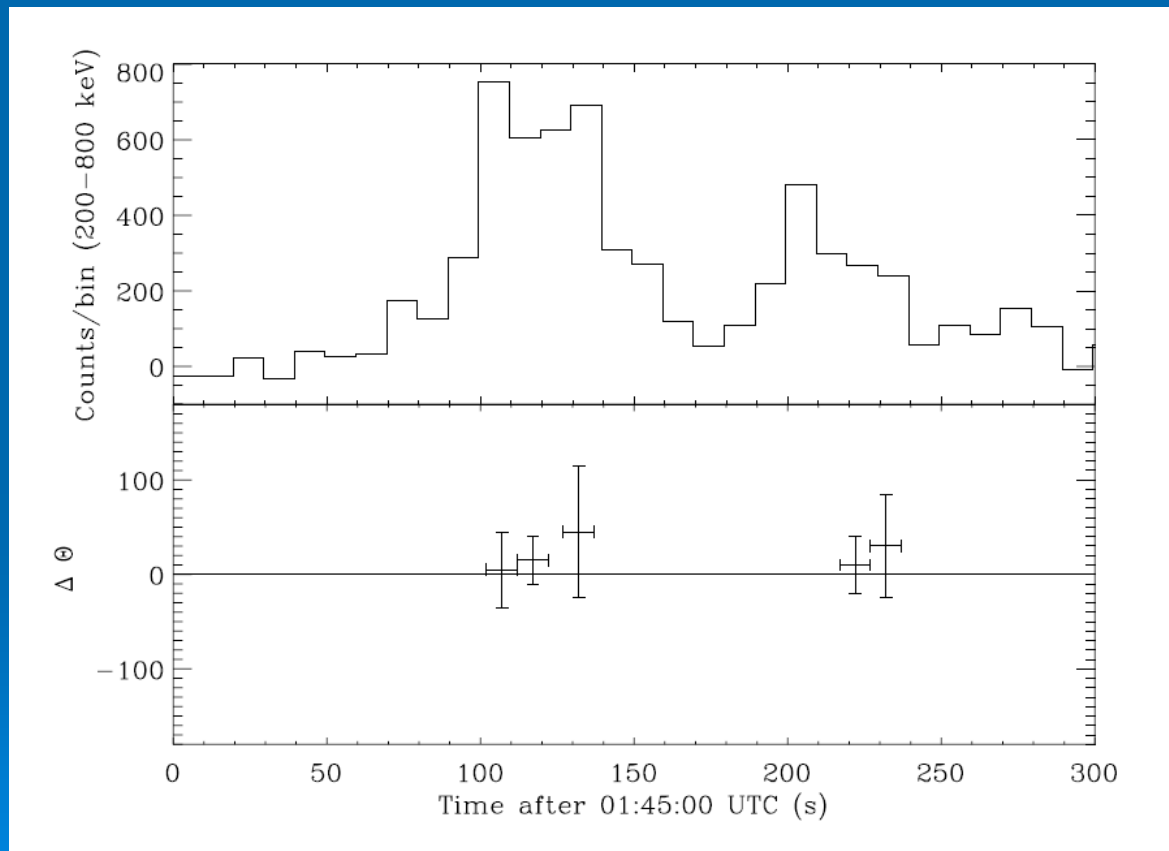


$\text{proba}(a > a_0, \text{ any } \varphi) = 0.06 \%$



GRB 041219A: constraints on LIV

Comparison of PA between 2 energy bands



200-250 keV
vs
250-325 keV
 $\Delta\theta = 21 \pm 47^\circ$

$$\Delta\theta(p) = \frac{\omega_+(k) - \omega_-(k)}{2} d \approx \xi \frac{k^2 d}{2M_{Pl}}$$

$$\xi < 4 \cdot 10^{-15}$$